# Ultracold molecules and ultracold chemistry

Tim Softley, Martin Bell

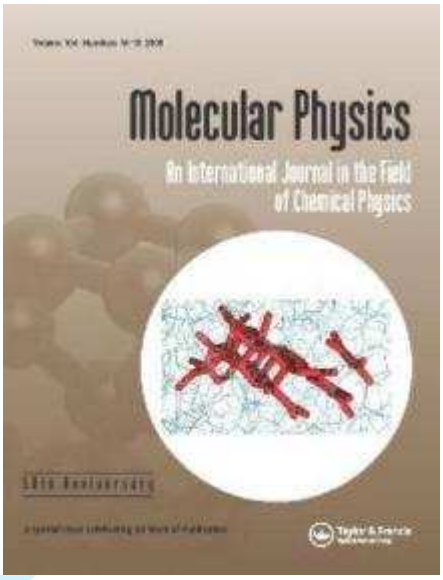


# Ultracold molecules and ultracold chemistry

| | |
|---|---|
| Journal: | *Molecular Physics* |
| Manuscript ID: | TMPH-2008-0416 |
| Manuscript Type: | Invited Article |
| Date Submitted by the Author: | 10-Dec-2008 |
| Complete List of Authors: | Softley, Tim; University of Oxford<br>Bell, Martin; University of Oxford, Department of Chemistry |
| Keywords: | Ultracold molecules |
| | |
| Note: The following files were submitted by the author for peer review, but cannot be converted to PDF. You must view these files (e.g. movies) online. | |
| cold_chemistry_review.tex | |

# Ultracold molecules and ultracold chemistry

Martin T. Bell and Timothy P. Softley*
*Department of Chemistry, University of Oxford*
*Chemistry Research Laboratory, Oxford OX1 3TA, UK*

The recent development of a range of new methods for producing samples of gas phase molecules that are translationally cold ($T \leq 1$ K) or ultracold ($T \leq 1$ mK) is driving efforts to study reactive and inelastic collisional processes in these temperature regimes. In this review article the new methods for cold/ultracold molecule production are reviewed in the context of their potential or current use in collisional studies and progress in the application of these methods is highlighted. In these sub-Kelvin temperature ranges, where the de Broglie wavelength is long compared to molecular dimensions, quantum effects may play a crucial role in the collision dynamics. Reactions with no potential energy barrier are of greatest importance, and this review article summarises some of the principal theoretical approaches to understanding quantum effects in these barrierless processes.

## I. INTRODUCTION

The remarkable progress in methods for producing, trapping and controlling ultracold atoms in the gas phase, based on methods of laser and evaporative cooling has been one of the major developments in physics in the late $20^{\text{th}}$ and early $21^{\text{st}}$ centuries [1]. Implementation of ever more sophisticated techniques for manipulating and studying ultracold matter using optical and electromagnetic fields is currently driving strong links with condensed matter physics [2] and the development of frameworks for quantum information processing [3]. Prompted by this success, principally with alkali metal atom systems, there has been a major effort to extend the methods of ultracold physics to include *molecular* species, for which laser cooling schemes are not generally applicable. This has led to the development of a new range of techniques that are capable of cooling molecules [4, 5]; in this article we review recent progress in the methods for producing cold and ultracold molecules and consider what these advances have to offer to chemistry. We also discuss how ultracold chemical collisions can be viewed from a theoretical perspective and report on current experiments that are being developed to study reactive and inelastic collisions at low temperatures.

In this field the word "cold" is generally used for temperatures ranging from 10 K to 1 mK, while "ultracold" implies sub-millikelvin temperatures, going down to the nanokelvin range and below, which are the domain of quantum degenerate gases such as Bose-Einstein condensates (BEC) [6]. In some senses, sub-Kelvin temperatures belong to an artificial world – the lowest temperatures observed in interstellar space are around 3 K [7, 8] – and little is known about chemical processes in this regime. But there is no doubt that this will be a world in which chemical dynamics will be dominated by quantum effects arising from the long de Broglie wavelengths of slowly moving molecules ($\lambda = h/p$ where $p$ is the momentum). Consider, for example, a room temperature gas of $CH_3F$ molecules where the mean molecular speed is around 400 $\text{ms}^{-1}$. At this velocity, the de Broglie wavelength associated with the translational motion of the molecules is around 0.03 nm, which is an order of magnitude smaller than the typical range of chemical interactions. At 30 mK, however, the mean speed is only 4 $\text{ms}^{-1}$ which gives a wavelength of 3 nm, now an order of magnitude larger than the range of intermolecular forces. Thus, while at room temperature the familiar notion of reactions occurring via classical collisions may be valid, at 30 mK the wave-like properties of the molecular motion are expected to be important.

The quantum nature of ultracold collisions may provide a detailed probe of fundamental chemical reactions. At higher temperatures, measurements of the rates of chemical processes are subject to a large amount of averaging which obscures the intricate details of molecular collisions. This is not only a consequence of the many internal rotational and vibrational quantum states typically occupied by the reactant molecules, but also the wide range of impact parameters, or angular momentum states, available to the collision partners. In contrast, at ultracold temperatures, averaging over quantum states is minimised; the populations of the internal quantum states collapse into the lowest one or two states and the collisional angular momentum becomes highly restricted, ultimately reaching the limit of a single active collisional angular momentum state (pure $s$-wave or $p$-wave scattering). Chemical reactions at low collision energies can also be profoundly influenced by the long-range intermolecular forces which control the orientation of the reactants during collisions [9, 10]. Experiments with cold molecules offer a way to sensitively probe this part of the intermolecular potential surface. Moreover, the weakness of these long-range interactions suggests that external fields are likely to exert a strong influence on the dynamics of chemical processes, potentially allowing fine control over the rates and outcomes of molecular collisions [11, 12]. For open-shell systems, multiple potential energy surfaces may converge to degenerate long range limits and therefore non-adiabatic interactions between these surfaces may play a crucial role in chemical dynamics. A final intriguing advantage of slowly moving molecules is that they can be trapped using optical, electrical or magnetic fields, allowing observation times for chemical processes that are very much longer than those available in conventional molecular beam experiments.

These considerations suggest that the sub-Kelvin world of chemical reactions will be one in which the refined control and detailed interrogation of chemical processes should be possible. Experimental measurements should provide considerable challenges to quantum theories of chemical reaction rates, both in the calculation of *ab initio* potential energy surfaces and the solution of the equations for quantum reactive scattering [13]. And although these temperatures lie well below those occurring naturally, studies of cold and ultracold chemical processes will ultimately provide a better understanding of thermally av-

*Electronic address: tim.softley@chem.ox.ac.uk

eraged dynamics at higher temperatures, for example in the 10 to 20 K range found in interstellar gas clouds [7].

In addition to the interest in applying ultracold techniques to reaction dynamics studies, there are a number of other potential applications. In high resolution spectroscopy, the long observation times and very narrow Doppler contributions to linewidths afforded by experiments with slowly moving [14] or trapped molecules [15] will allow measurements of exceptional precision. Molecular systems in particular offer opportunities to perform measurements relevant to fundamental physics; *e.g.*, searches for an electric dipole moment of the electron [16], parity-violation in chiral molecules [17] or the time variation of fundamental constants [18, 19]. There is also considerable interest in producing new types of quantum degenerate molecular gases to enrich the toolkits currently being used to explore fundamental many-body and condensed matter physics [20, 21]. Chemical reactions occurring in these exotic phases of matter, such as BECs or Fermi-degenerate gases, where the de Broglie wavelength may be comparable with inter-molecular separation, may also be enhanced or suppressed by many-body quantum effects [22–24]. Finally, the trapping of ultracold dipolar molecules, particularly in optical lattices, may be an important way forward in the development of quantum information processing schemes [25, 26].

In Section II of this paper we introduce some basic concepts of barrierless chemical processes and the capture theory approach to describing the dynamics. In Section III we review the wide-ranging methods that have been developed to produce translationally cold or ultracold molecules, while in Section IV the different methods to trap such cold samples using electromagnetic fields are described, together with the secondary cooling techniques that might be applicable to the trapped samples. In Section V some recent progress in using these cold/ultracold molecule sources for collisional studies is reviewed, while Section VI provides an introduction to the theoretical description of ultracold collisions. Finally we sum up progress to date in Section VII and consider future prospects for development of applications in this field.

## II. LOW-TEMPERATURE CHEMISTRY

How does chemical reactivity change at very low collision energies? Many familiar gas phase chemical reactions occur as thermally activated processes and their behaviour can be well understood using transition state theory [27]. For these reactions, in which reactants are separated from products by an activation barrier, thermal energy is needed before the reactants are able to pass through a transition state on the reaction potential energy surface prior to forming products. At low temperatures, the thermal fluctuations that produce collisions with sufficient energy for reaction become increasingly rare, and so the rate constants predicted by classical theory become vanishingly small. For even the most modest of barriers, the Arrhenius-like dependence of the rate constant prevents most chemical reactions from occurring at low temperatures [28]. Exceptions may arise from quantum mechanical tunnelling which in certain reactions involving light atoms may allow transmission though the reaction barrier at much lower energies. For the moment, however, our interest will focus on a different class of reactions: those which have no potential energy barrier along the reaction coordinate.

These "fast chemical reactions" [29] frequently have very large bimolecular rate constants at room temperature and exhibit profoundly non-Arrhenius behaviour as the temperature is lowered. They typically occur in highly reactive systems and often play a central role in a variety of astrochemical, combustion, plasma and photochemical processes. Table I lists examples of some of these "barrierless" reactions (while not all of the reactions falling into these categories will be barrierless, it is possible to find many examples which behave this way). In many cases we have been able to choose examples in which one or more of the reactants might be produced at low temperatures using currently existing experimental techniques, as described in Section III. Of particular interest in the context of astrochemistry are reactions such as those occurring in bimolecular collisions between $H_2$ molecules and $H_2^+$ molecular ions (which is the most abundant reaction in the universe) or barrierless reactions involving carbon atoms, which are thought to provide a mechanism for lengthening carbon chain molecules in interstellar space.

A distinguishing feature in these types of system is the existence of deep wells on the reaction potential energy surface which represent short-lived chemical complexes (see Fig. 1a). The formation of these intermediates, which often occurs by insertion of an atom or molecule into a chemical bond, represents a different fundamental mechanism from the transition state model often used to describe reactions with an activation barrier. In this case, the results of molecular collisions are strongly influenced by the long range intermolecular forces which control the orientation of the approaching reactants.

The collision dynamics for a barrierless process can be most easily understood in terms of motion on an *effective potential* which accounts for the conservation of angular momentum during the collision. For an intermolecular potential described by an inverse-power law (which ignores any angular anisotropy), this effective potential becomes

$$V_{\rm eff}(r) = \frac{b^2 E_c}{r^2} - \frac{C_s}{r^s}, \qquad (1)$$

where $E_c$ is the collision energy, $r$ is the separation between the collision partners and $b$ is the impact parameter for the collision (the distance of closest approach in a given trajectory were the molecules undiverted by the intermolecular potential) which is related to the orbital angular momentum ($l$) for the collision via;

$$l = \mu v_{\rm rel} b. \qquad (2)$$

The first term in Eq. 1 represents the centrifugal force that prevents the close approach of the colliding molecules necessary for reaction to occur. Thus, even for intermolecular potentials that have no chemical barrier separating reactants from products, there may be an $l$-dependent barrier associated with the orbital motion of the colliding molecules.

In many capture theory approaches to calculating cross sections, it is often assumed that the radial motion (along the reaction co-ordinate) may be described classically and that only trajectories that surmount the centrifugal barrier go on to form products (with unit probability). This then leads to the definition of a maximum impact parameter for successful collisions, $b_{\rm max}(E_c)$, and allows the *Langevin*

TABLE I: Selected examples of barrierless processes

| Barrierless process | Examples | Refs. |
|---|---|---|
| Atom-molecule reactions | $O(^3P) + OH(X^2\Pi) \rightarrow O_2(X^3\Sigma_g^-) + H(^2S)$ | [30, 31] |
| | $C(^3P) + C_2H_2 \rightarrow C_3H + H$ | [32, 33] |
| Ion-neutral reactions | $H_2^+ + H_2 \rightarrow H_3^+ + H$ | [34] |
| | $Ca^+ + CH_3F \rightarrow CaF^+ + CH_3$ | [35] |
| | $NH_3{}^+ + ND_3 \rightarrow NH_3D^+ + ND_2$ | [36] |
| Radical reactions | $CH(X^2\Pi) + D_2 \rightarrow CD(X^2\Pi) + HD$ | [37] |
| | $CN(^2\Sigma^+) + O_2(^3\Sigma_g^-) \rightarrow NCO + O$ | [38] |
| | $SO(^3\Sigma^-) + OH(^2\Pi) \rightarrow SO_2 + H$ | [39, 40] |
| | $HBr + OH(^2\Pi) \rightarrow H_2O + Br$ | [41] |
| Reactions of electronically or vibronically excited molecules (including Rydberg states) | $Ne^* + NH_3 \rightarrow Ne + NH_3^+ + e^-$ | [42, 43] |
| | $H_2(n = 30\text{–}70) + H_2 \rightarrow H_3^* + H \rightarrow H_3^+ + e^-$ | [44, 45] |
| | $RbCs + RbCs \rightarrow Rb_2 + Cs_2$ | [46] |
| Unimolecular decomposition | $SO_2 + h\nu \rightarrow [SO_2]^* \rightarrow SO + O$ | [47, 48] |
| | $H_2CO + h\nu \rightarrow [H_2CO]^* \rightarrow HCO + H$ | [49] |

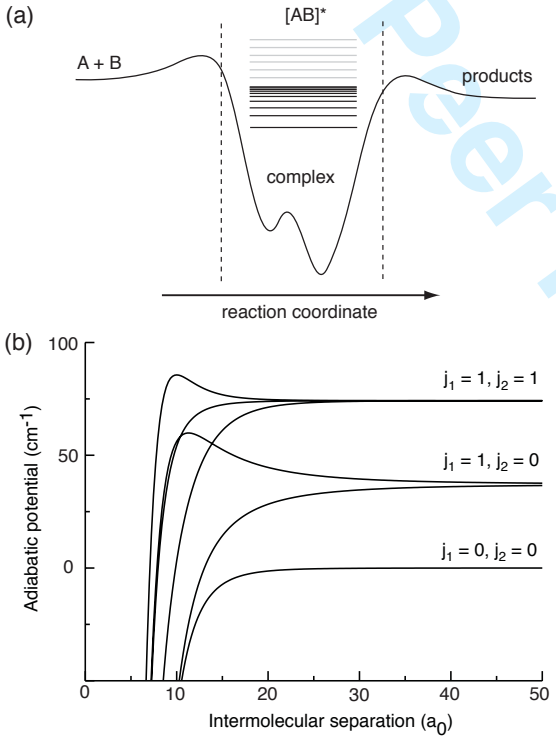


FIG. 1: (a) Reaction profile for a "barrierless" reaction. The long-range intermolecular potential and centrifugal potential control the dynamics of complex formation. In addition to the many bound states supported by the deep potential well there are many short-lived states which can decay to form products. (b) Examples of adiabatic potential curves for two polar molecules with parameters chosen to resemble those of OH molecules. The curves shown are for $J = 0$ and the rotational quantum numbers of the free molecules are denoted $j_1$ and $j_2$.

cross section for the reaction to be calculated as:

$$\sigma_L(E_c) = \pi b_{\max}^2(E_c), \tag{3}$$

which, for the intermolecular potential of Eq. 1, can be written

$$\sigma_L(E_c) = \pi \left(\frac{s}{s-2}\right)^{1-2/s} \left(\frac{sC_s}{2E_c}\right)^{2/s}. \tag{4}$$

When integrated over a thermal distribution of collision energies, this integral cross section gives a thermal rate constant for the reaction which varies as [29],

$$k(T) \sim T^{(1/2-2/s)}. \tag{5}$$

This temperature dependence is markedly different from the Arrhenius behaviour expected for reactions possessing a barrier and reflects the competition between the collision frequency (which decreases at low temperatures) and the capture probability (which increases at low temperatures). For $s = 4$, the rate constant is actually independent of temperature. This case is encountered for reactions occurring between an ion and a non-polar molecule (a charge induced-dipole interaction), and such behaviour has been found experimentally over a wide range of temperatures [50].

Clearly, this simple approach neglects many of the details of the reaction. The assumption of an isotropic intermolecular potential ignores effects from the rotation of the colliding molecules and the orientation-dependence of their interaction. To correct this, more detailed calculations can be performed to produce radial potential curves that depend on the initial rotational quantum states of the molecules. This approach forms the basis for the rotationally adiabatic capture theory developed by Clary [29, 51] and also the statistical adiabatic channel model of Troe and co-workers [52]. Both these methods also take into account quantisation of the total angular momentum, the effects of which become increasingly important at low temperatures. Examples of the adiabatic potential curves which govern the capture dynamics are shown in Fig. 1(b), for the case of two polar molecules.

Capture-based approaches have been remarkably successful in describing the temperature dependence and the absolute magnitudes of rate constants for barrierless ion-molecule collisions down to temperatures of around 10 K [53]. However, in order to describe the reaction purely in terms of long-range intermolecular forces, it is important that the positions of the centrifugal barriers are located at large intermolecular separations. Whilst this is likely to be the case for ion-molecule reactions, collisions between neutral molecules will sample the shorter range parts of the potential surface where chemical forces become im-

portant. As such, for most chemical reactions, extensive *ab initio* electronic structure calculations are required and, for open-shell reagents, further complications arise from the possibility of reaction on multiple potential energy surfaces [54].

Although we have described the rates of barrierless chemical reactions using a classical capture approximation, it is likely that the assumption of classical motion along the reaction co-ordinate will become a poor approximation in the cold and ultracold regimes, as discussed in more detail in Section VI of this paper. Fully quantum mechanical reactive scattering calculations are possible for certain barrierless reactions, although such calculations are particularly demanding as a large number of basis functions are required to describe the many quantum states supported by deep potential wells. In spite of this, there have been a number of impressive quantum dynamics calculations on systems involving three-atoms. For example, Launay and co-workers have used a time-independent hyperspherical close-coupling method to calculate reaction and inelastic cross sections for atom exchange reactions involving alkai-metal atoms and dimers and also for various insertion reactions [55]. One area where such calculations are particularly useful concerns the trap stability of highly vibrationally excited dimers formed by photoassociation (see Sections III and IV):

$$\mathrm{M}_2(\nu) + \mathrm{M} \rightarrow \mathrm{M}_2(\nu' < \nu) + \mathrm{M}, \qquad (6)$$

where M = Li, Na, K. The exothermicity of these vibrationally inelastic collisions is more than sufficient to eject the molecules from the trap.

The astrophysical importance of barrierless reaction processes at temperatures as low as 10 K has driven the development of experimental methods for measuring reaction cross sections down into this temperature range. Most notably, the rapid expansion of a high-pressure gas through a small hole into vacuum has proved to be a particularly powerful and versatile method for producing cold molecules. Multiple collisions between molecules in an expanding supersonic jet produce a fast-moving supersonic molecular beam with a narrow velocity distribution and significantly cooled internal degrees of freedom [56]. Translational temperatures below 1 K can routinely be obtained for motion defined in the frame of reference moving at the mean beam velocity, limited only by the formation of clusters and by finite collision cross sections. Molecules with higher perpendicular velocity components can be eliminated from the beam using skimmers. The thermodynamic price associated with the formation of such low-temperature beams is a high laboratory frame velocity (as the expansion occurs adiabatically, the thermal enthalpy is converted to kinetic flow energy). As a consequence, crossed molecular beam experiments are unable to achieve very low collision energies even at small crossing angles as the mean velocities of the beams contribute to the effective collision energy and because the energy resolution becomes limited by the spread of velocities in the beams. Only by seeding two chemical species into a single beam under conditions where collisions may still occur can low temperature reactions be achieved. In this way, Smith and co-workers demonstrated that low collision-energy ion-molecule reactions could be studied by ionizing one species in the high density part of the molecular beam [57]. Similarly, Mackenzie *et al.* in their study of the $H_2^+ + H_2$ reaction [34] demonstrated the possibility of accelerating an ionized species within a supersonic beam to induce collisions with the neutral molecules.

Much greater control of the temperature can be achieved in the CRESU experiment (as reviewed in Refs. [53, 58]) in which a large diameter Laval nozzle is used to obtain genuine thermal equilibrium within a supersonic beam at temperatures as low as 7 K, but more typically down to 15 K. Reactive species are generated either by pulsed laser photolysis or photoionization within a helium beam using a high backing pressure and high densities ($\sim 10^{16}$ molecules cm$^{-3}$). Reactive collisions in the jet occur in the 100–500 $\mu$s during which the flow remains uniform. A wide variety of reactions have been studied using this technique and absolute values for the thermal reaction rate constant can be obtained as a function of temperature; for example, Carty *et al.* have studied the reaction of CN + allene over the 10–100 K range [59].

The primary experimental challenges for studying reactions in the *sub-Kelvin* range are the development of general methods for decelerating and cooling molecules, and finding techniques that produce sufficient molecules to detect reaction products. Currently, a number of methods, which are discussed below, exist which might typically generate number densities of the order of $10^8$ molecules cm$^{-3}$. But consider a hypothetical experiment in which samples of two reacting species have been brought together with these densities. For collisions with a relative velocity of 1 ms$^{-1}$ and a collision cross section of $10^{-15}$ cm$^2$, the collision frequency per molecule ($Z = \sigma v_{\mathrm{rel}} N$) would be just $10^{-5}$ s$^{-1}$. The density of product molecules, assuming they could be trapped in the same volume as the reactants, would then initially increase at a rate of only $10^3$ cm$^{-3}$ s$^{-1}$. It is apparent from these figures that either very long interaction times are required to study reactive collisions or that somewhat higher densities are needed to make the detection of products viable. In Section V we highlight the advantages of studying ion-molecule collisions in this respect.

## III. TECHNIQUES FOR MAKING COLD AND ULTRACOLD MOLECULES

The success of many experiments with ultracold atoms arises ultimately from the use of laser cooling to obtain high densities of trapped atoms at temperatures of around 1 mK and below [60]. Laser cooling or the manipulation of atomic motion by optical fields can occur by several mechanisms, one of which is the scattering force produced by a radiation field resonant with an atomic transition [60]. This force provides the basis for Doppler laser cooling whereby an atom irradiated with laser light detuned slightly below an atomic transition frequency is cooled by repeated cycles of stimulated absorption and spontaneous emission. In each cycle, atoms moving towards a laser beam may absorb a photon as a consequence of the Doppler shift and the momentum of the absorbed photon produces a recoil which slows the atom. As the atom returns to the ground state by spontaneous emission (which in free space has no preferred direction), the average effect over many cooling cycles is a viscous force which damps the atomic motion. Large cooling rates require a closed two-level transition with a short excited state lifetime and for this reason, optical transitions in alkali metal atoms, metastable rare gas atoms or singly-charged alkaline-earth metal ions are most frequently used. Unfortunately, for

reasons discussed below, the dense and complicated energy level structure present in molecular systems has so far prevented the direct use of laser cooling techniques to obtain low temperature molecules. Instead, a wide variety of alternative methods have been developed in many different laboratories. In this section we review these methods and their prospects for studying ultracold chemical reactions.

The problem with laser cooling molecules, or atoms with more complicated energy level structures, is that spontaneous emission can occur into metastable states that no longer interact with the cooling lasers. In atomic systems this "shelving" of the population can often be addressed with additional lasers which repump these states back into the optical cooling cycle. For molecules, however, such an approach is impractical because fluorescence can occur over a range of wavelengths, which ensures the population is distributed over a large number of rovibrational states, each requiring a repumping laser tuned to the correct frequency [61]. As rotational transitions typically occur with well-defined selection rules, the difficulty arises mainly from the lack of vibrational selectivity. Several schemes have been suggested to overcome this problem [61–64]: for example, choosing a diatomic molecule with a nearly-diagonal Franck-Condon matrix or using optimally-shaped femtosecond laser pulses in the excitation step, but these have yet to be tested.

Laser cooling can still be used to obtain cold molecules by an indirect route: the coldest molecular gases produced in the laboratory to date have been formed through the pairing of ultracold alkali metal atoms by three-body collisions, photoassociation or magnetic Feshbach resonance tuning. However, the search for alternatives to laser cooling has led to the development of experimental techniques which are able to produce low-temperature molecules of greater chemical diversity. These include various methods for decelerating molecules in a molecular beam, such as Stark, Zeeman or optical deceleration; buffer gas cooling; collision-based cooling and velocity selection. Figure 2 shows the typical temperatures and number densities that can be produced by these various sources of cold molecules. Molecules such as $ND_3$, NO, $CH_3F$, or radicals such as OH and NH, can now be produced with temperatures in the millikelvin range and, in the cases of Stark deceleration and buffer gas cooling, electrostatic and magnetic trapping has been achieved. In contrast with the techniques using ultracold atoms, the number densities obtained at these temperatures are typically limited to around $10^8$ molecules $\mathrm{cm}^{-3}$. This limitation arises mainly because conservative forces are used to manipulate the molecules and so the phase space density remains constant, as required by Liouville's theorem. For molecules with a thermal de Broglie wavelength $\Lambda = (2\pi\hbar^2/mk_{\mathrm{B}}T)^{1/2}$, the phase space density can be written,

$$D = n\Lambda^3, \tag{7}$$

where $n$ is the number density. This parameter provides a measure of the quantum wavelength of the molecules in terms of their average intermolecular separation; as $D$ increases the fundamental distinguishability between molecules diminishes until eventually quantum degeneracy is reached. Liouville's theorem dictates that the phase space density remains constant for a system of particles evolving under the action of forces which do not depend on their velocities (*i.e.*, those described by a classical Hamiltonian). Genuine cooling can only be brought about by the action of dissipative forces and so, for techniques based on decelerating a molecular beam, the maximum possible phase space density is limited to that obtained after the initial supersonic expansion. Thus, although trapping of neutral molecules has now been achieved by a number of groups, the challenge of obtaining simultaneously colder and more dense ensembles of molecules will require secondary cooling schemes to be developed (see Section IV).

### A. Molecular beam deceleration

#### 1. *Stark deceleration*

Just as electric fields have been used for many years in accelerator physics to control the velocity of charged particles, they can also be used to manipulate the motion of polar molecules. This idea has provided the motivation for the Stark decelerator, a device designed and first implemented by Meijer and co-workers [65, 66] that uses time-varying electric fields to bring part of a supersonic molecular beam to rest in the laboratory frame. The principle employed is illustrated in Figs. 3(a) and (b). The molecular beam passes through a series of high voltage electrode pairs, designed to create large inhomogeneous electric fields along the decelerator axis. As molecules enter the region of high electric field between the electrodes, those in "low-field seeking" quantum states (for which the Stark effect produces a positive shift of energy with field) gain potential energy at the expense of kinetic energy and become fractionally slowed. For a static electric field configuration, these molecules would subsequently be accelerated away from the electrodes after passing the field maximum, but switching the high voltages to the next pair of electrodes allows the kinetic energy to be permanently removed. This process is repeated along the length of the decelerator and each pair of electrodes also acts as an electrostatic lens to allow transverse focussing of the beam. Figure 3(c) shows a typical time of flight spectrum produced using a 131-stage Stark decelerator in our own laboratory following deceleration of $ND_3$ molecules seeded in a xenon molecular beam.

Even when light molecules are seeded into a beam of a heavy carrier gas such as xenon, approximately 100 $\mathrm{cm}^{-1}$ of energy must be removed for deceleration to near-zero velocity. A polar molecule in a quantum-state with an effective dipole moment of 1 D, experiencing a change in electric field of 100 kV/cm, loses less than 2 $\mathrm{cm}^{-1}$ of Stark energy. This means the deceleration process must be repeated over many stages, using a precisely timed pulse sequence to match the high-voltage switching to the decreasing molecular velocity. The motion of the ensemble of molecules in the time-varying fields inside the Stark decelerator has been analysed in some detail [67–69], with the result that only a "phase-stable" fraction of the initial molecular beam can actually be decelerated. In particular, only molecules which have suitable positions and velocities at the start of the switching sequence, and which are in the correct quantum state, are found to undergo large changes in their motion. These state-selected molecules exit the decelerator as a small packet (or packets), a few millimeters in length, with a very narrow velocity distribution centred around a tunable final velocity [70]. In addition to trapping and reflection of the decelerated packet, full 6D manipulation of the phase space distribution has

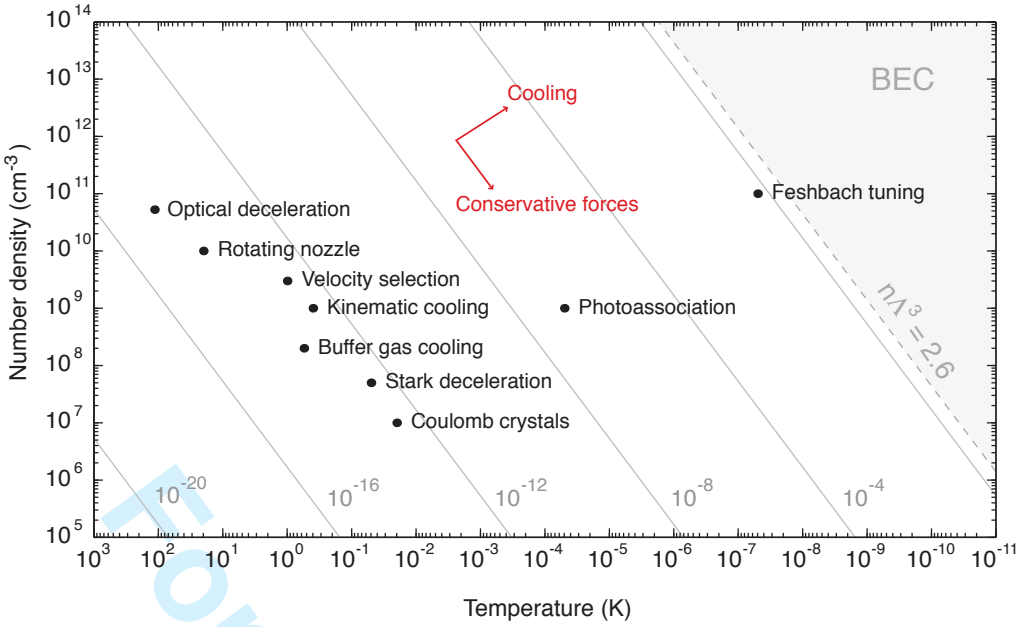


FIG. 2: Current techniques for producing cold molecules. The quoted number densities and temperatures are rough guides based on reported experimental measurements; they do not necessarily reflect limiting values for each technique. The grey lines indicate contours of constant phase space density for a small molecule (ignoring the distribution of the population over different internal states).



been demonstrated using focussing hexapoles and a bunching device, which has allowed the creation of molecular beams with effective longitudinal temperatures as low as 250 $\mu$K [71].

Slowly moving molecules produced using this technique have already found many applications, including: high-resolution spectroscopy [14, 18] and lifetime measurements [72, 73]; trapping in static and AC electric fields [74–78]; magneto-electrostatic and magnetic trapping [79]; reflection from a microstructure or permanent magnet array [80, 81] and tunable-energy collision studies [82]. More recently, a molecular synchrotron [83] has been constructed which confines molecules in bunches orbiting inside a split hexapole ring – a direct analogue of the charged-particle synchrotrons used for high-energy collision experiments. The Stark deceleration technique is best suited to light molecules with large first-order Stark shifts and, to date, has been demonstrated for a number of molecules in low-field seeking states: metastable CO ($a^3\Pi$) [65, 73]; $ND_3$ and other ammonia isotopomers [84]; OH/OD ($X^2\Pi, \nu = 0, 1$) [75, 85–87]; formaldehyde [88]; NH ($a^1\Delta$) [76, 89], $SO_2$ [47, 48]. There is also the interesting possibility of creating cold SO molecules and oxygen atoms by near-threshold photodissociation of decelerated $SO_2$ molecules. For this purpose, a 326-stage decelerator has been constructed and successfully tested in the group of Tiemann [48]. Applications of Stark decelerated molecular beams have recently been reviewed by van de Meerakker *et al.* [90]. Current work in our lab is focussed on decelerating $CH_3F$ / $CH_2F_2$ molecules and generating radicals such as CH ($X^2\Pi$) for deceleration.

A different design of Stark decelerator can also be used to slow beams of molecules in *high-field seeking* states (those for which the energy decreases with increasing field strengths) [91] and proof of principle experiments to decelerate metastable CO [92], benzonitrile [93], OH [94] and YbF [95] have been demonstrated in the groups of Meijer and Hinds. Deceleration of molecules in high-field seeking states is necessarily more challenging as the molecules can only be prevented from crashing into the high-voltage electrodes using dynamic or "alternate gradient" (AG) focussing schemes which only provide relatively weak transverse confinement [96]. However, these techniques are particularly important as they allow polar molecules to be decelerated in their ground rotational state (which is always high-field seeking) and because they can be used to slow heavy molecules of spectroscopic or biomolecular interest (which generally do not have suitable low field seeking states). An extensive review of AG focussing and deceleration is given in Ref. [96], and an analysis of how to optimise the transverse dynamics during AG guiding is provided in Ref. [97]. One of the advantages of producing decelerated ground state molecules is that these are not subject to energy releasing inelastic collisions, thus enhancing prospects for sympathetic cooling by elastic collision (see Section IV).

Stark decelerated molecular beams offer potential advantages for chemical reaction studies: they are intrinsically quantum state-selected, and have arbitrarily tunable final speeds and narrow velocity distributions. Consequently, they are well-suited to precise measurements of the energy-dependence of scattering cross sections and the possibility of electrostatic focussing using pulsed hexapole fields could allow targeted collision experiments with trapped ions, laser-cooled atoms or with surfaces.

### 2. *Zeeman deceleration*

In direct analogy with the Stark decelerator, Vanhaeke and Merkt [98], and subsequently Raizen and co-workers [99] have demonstrated that pulsed inhomogeneous magnetic fields can be used to decelerate molecules and atoms with magnetic dipole moments. Vanhaeke and Merkt used a six-stage (and subsequently a 12-stage [100]) decelerator to reduce the energy of ground state H atoms by 50% (and also later to decelerate D atoms [100]), while Raizen and co-workers have used an 18-stage decelerator

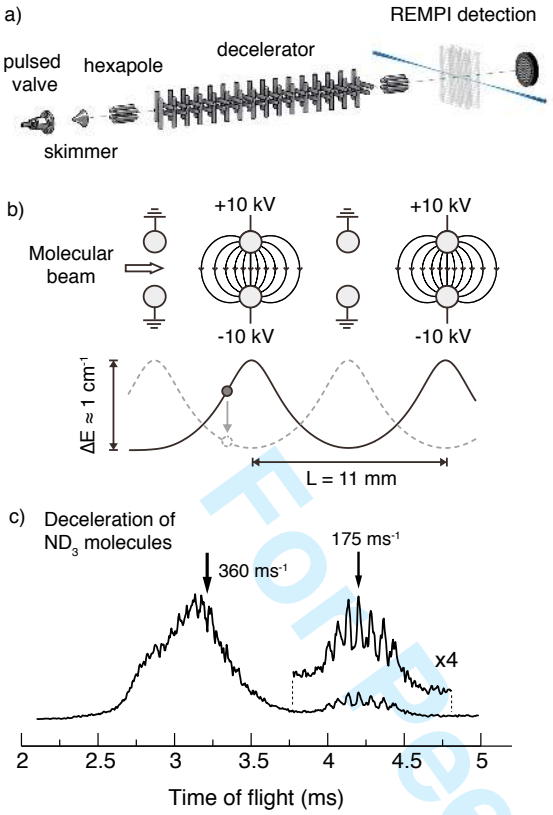


FIG. 3: a) Experimental setup for Stark deceleration b) Principle of Stark deceleration. Molecules in low-field seeking quantum states lose kinetic energy as they enter regions of high electric field between the high voltage electrodes. As the molecules near the top of the potential energy curve, the high voltages are switched to the next pair of electrodes, removing energy from the beam. This process is repeated along the length of the decelerator. c) Experimental time of flight spectrum for slowing $ND_3$ molecules using our 131-stage Stark decelerator. The central packet of the late-arriving molecules has been decelerated from 360 $ms^{-1}$ to 175 $ms^{-1}$, removing around 75% of the kinetic energy.

to slow a beam of metastable neon atoms from 461 $ms^{-1}$ to 403 $ms^{-1}$ [101]. In both cases, a pulsed high current is passed though water-cooled electromagnetic coils to generate magnetic field strengths of several Tesla. For these field strengths the amount of kinetic energy lost per switching stage is generally similar to that in Stark deceleration and the same principles of phase-stability apply. This approach offers exciting prospects for decelerating free radical species for chemical reaction studies; for example, the Zeeman deceleration of molecular oxygen has recently been demonstrated using a 64-stage decelerator [102]. As the time sequence for pulsing the magnetic fields depends on the specific Zeeman shifts of the molecules, the slowed molecules are intrinsically state-selected (as with Stark deceleration). Magnetic trapping of Zeeman-decelerated H atoms has also recently been reported [103], and similar experiments with other atoms and molecules can be anticipated.

### 3. *Rydberg deceleration*

When a molecule is excited to a high Rydberg state with one electron in an orbit of high principal quantum number (*e.g.* $n = 10 - 100$) the electron distribution is highly polarizable. In an external electric field, the electronic eigenstates of the molecule show a large linear Stark shift, and there is a lifting of the very high electronic degeneracy of Rydberg states (arising from the many $l$ and $m_l$ states of given $n$). The states whose energy increases with the field strength have electron distributions in which the Rydberg electron is localised on the side of the atom pointing away from the field direction. Conversely, those states whose energy decreases with field have the electron localised on the side pointing in the direction of the field. In either case a large dipole moment is created which can be of the order of $n^2$ atomic units – many orders of magnitude greater than in a typical ground state molecule. Thus, in principle, molecules in Rydberg states are much more readily decelerated by inhomogeneous electric fields.

Softley and co-workers demonstrated that a single-stage dipole, produced by a pair of cylindrical rods, with fields of the order of 1 $kVcm^{-1}$, (compared to 100 $kVcm^{-1}$ in the Meijer-type Stark decelerator) could reduce the energy of an $H_2$ Rydberg beam ($n \sim 20$) by 10% [104, 105]. Subsequently, Merkt and co-workers demonstrated that two pairs of electrodes could be used to bring H atoms ($n \sim 30$) to a standstill, and subsequently reflected [106] or electrostatically trapped [107, 108]. There are several complications with this technique, however, the main one being associated with the lifetime of these highly excited species. In the experiments of Softley *et al.* with $H_2$ molecules, these lifetimes were around 5 $\mu$s, while for the H atom experiments the higher-$n$ states survived for more than 10 $\mu$s. The fields that are applied to decelerate the molecules can have major effects on the lifetimes of the Rydberg states, and the need to preserve long lifetimes sometimes conflicts with the optimum fields for deceleration. Thus for example, it has been shown that populating Rydberg states in the presence of a field and then switching that field to zero generates long-lived states. However, near zero-field the high-field or low-field seeking character of the states is likely to be scrambled, hindering deceleration. A significant difference between atoms and molecules in this respect is that predissociation does not exist for atoms, whereas it dominates for molecules. Consequently, the main decay processes for atoms are spontaneous emission and stimulated absorption/emission by the black-body radiation field. Other complications include the energy level crossings between the numerous Rydberg states at specific fields. If these crossings are followed adiabatically by the molecule then a low-field seeking state can be converted instantaneously into a high field seeking state (and vice versa)[109]. A decelerative process may then suddenly become accelerative and the molecules become attracted to the electrodes.

There are potentially interesting applications of cold Rydberg states – not only in their chemistry, where they may react with neutral ground states rather like ion-molecule reactions, but also in electron transfer processes with electron-acceptor molecules like $SF_6$ [45]. There is also considerable interest in the properties of ultracold Rydberg gases, and it has been suggested that these might be suitable for quantum computing applications [110, 111]. Greene *et al.* have also suggested the existence of exotic molecules formed by interaction between a Rydberg atom and a ground state atom [112]. The wavefunctions of the species have inspired the name "trilobite" states because their multimodal characteristics resemble the fossils of these now extinct animals.

#### 4. *Optical deceleration*

Neutral molecules can also be decelerated through their interaction with far-off-resonant optical fields. This "optical Stark deceleration" makes use of the very large electric fields that can be generated using pulsed lasers: through the second-order Stark effect, polarizable molecules in a laser focus experience an induced-dipole force for the duration of the laser pulse. For non-oriented molecules, the optical field in a non-resonant laser pulse produces a quasi-electrostatic potential [113],

$$U(\mathbf{r},t) = -\frac{1}{4}\alpha\,|E(\mathbf{r},t)|^2, \qquad (8)$$

where $\alpha = (\alpha_{\parallel} + 2\alpha_{\perp})/3$ is the polarizability averaged over all orientations of the molecular axes and $E(\mathbf{r},t)$ is the time- and space-dependent electric field, which is averaged over one optical cycle. This potential is such as to draw molecules into the high-field region and the resultant force can be used to accelerate/decelerate, separate, focus or trap molecules [114–118] with appropriate optical field configurations. As the induced-dipole interaction depends only on the molecular polarizability, the method is potentially very general, although multiphoton/tunnelling ionization and molecular photodissociation processes limit the intensity of laser pulse that can be used [119].

Barker and co-workers have used a travelling optical lattice formed by the interference of two counter-propagating laser pulses to decelerate seeded molecular beams of NO and benzene [120, 121]. By changing the lattice velocity, laser intensity and pulse duration, the molecules could be tunably accelerated or decelerated. The experimental setup is illustrated in Fig. 4. In the case of NO molecules, nanosecond pulses with intensities of around $10^{11}$ W/cm$^2$ from two Nd:YAG lasers, were used to create a lattice with an average well depth of 22 K moving with a constant velocity of 321 ms$^{-1}$. For this choice of parameters, the NO molecules undergo a half-oscillation in the travelling potential wells, producing a deceleration from 400 ms$^{-1}$ to 270 ms$^{-1}$. Although only $10^5$ molecules per pulse are slowed, their density of around $10^{10}$ molecules cm$^{-3}$ is comparatively high and these values might be further increased by moving the laser focus closer to the molecular beam nozzle [120]. Ramirez-Serrano *et al.* have also shown the acceleration and deceleration of $H_2$ molecules by up to 200 ms$^{-1}$ using a stationary interference pattern at high-intensities [122].

#### 5. *Mechanical slowing methods*

A conceptually simple approach to generate cold molecules with low lab frame velocities involves rapidly moving a molecular beam source backwards as the gas expands forwards, allowing direct cancellation of the flow velocity of the beam. This kind of mechanical manipulation of beam speeds was originally developed by Moon *et al.* for beam acceleration [123], but more recently Herschbach and co-workers have been able to demonstrate the slowing of a supersonic beam emerging from the tip of high-speed rotor [124, 125]. By varying the rotor frequency, the speed of the beam as it exits the counter-rotating nozzle can be tunably increased or decreased. As this technique is very general it is potentially useful for chemical dynamics studies. It has been shown to work for

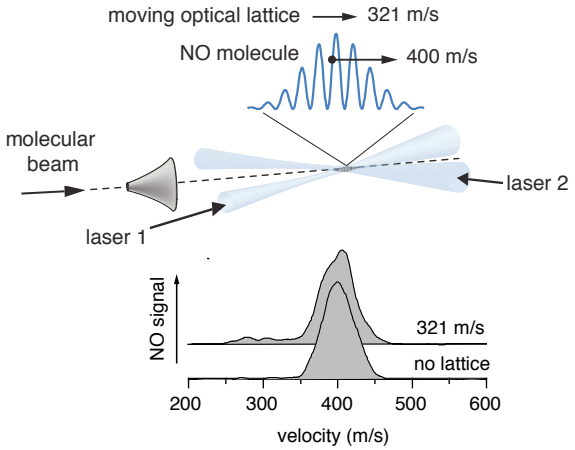


FIG. 4: Optical Stark deceleration. The velocity of the moving optical lattice is chosen to be lower than that of the molecular beam, allowing the molecules to be trapped in the travelling well created by the optical potential. The molecules are decelerated by a "half-rotation" in phase-space in the few nanosecond duration of the pulses. Experimental results adapted from Fulton *et al.* [121].

molecules such as $O_2$ (lowest velocity 67 ms$^{-1}$), $CH_3F$ (91 ms$^{-1}$) and $SF_6$ (55 ms$^{-1}$). However, a number of technical difficulties exist: Most significantly, the very large centrifugal forces in the rotor make the design of a pulsed system very challenging and, in the experiments of Herschbach and co-workers, the gas emerged continuously from the rotor tip as a 360° spray, limiting the beam intensity and generating a large background pressure.

A second method which makes use of fast mechanical motion in the laboratory frame has been developed by Raizen and co-workers [126]. By mounting a silicon wafer at the tip of a large diameter, high-speed rotor, a supersonic beam of helium atoms was reflected from the fast-receding crystalline surface. In much the same way as a tennis player slows a tennis ball with a drop shot, the reflected He atoms could be decelerated from 511 ms$^{-1}$ to 265 ms$^{-1}$, with the final velocity limited by the maximum rotor speed. The velocity spread of the slowed beam was found not to have significantly increased following the specular reflection. It remains to be seen whether the technique can be extended to decelerate light molecules such as $H_2$, $D_2$ and $CH_4$.

### B. Velocity selection

In a sample of gas at around room temperature there exists a broad Maxwell-Boltzmann distribution of velocities, which includes a certain fraction of molecules with very low speeds. Although this fraction is small – typically only 0.1% of molecules have speeds less than 10% of the mean – the total number of slowly moving molecules can still be high and these molecules can be extracted as a source of "cold" molecules. Experiments by Rempe and co-workers [127, 128] have demonstrated that for certain dipolar molecular gases, a high-voltage electric quadrupole with a right-angle bend can be used to filter the low-velocity molecules from a room-temperature gas injected at low pressure from an effusive nozzle (as illustrated in Fig. 5(a)). For molecules in low-field seeking quantum states, the large inhomogeneous

electric fields in the quadrupole guide create a conservative two-dimensional trapping potential which confines the slow moving molecules between the electrodes, allowing them to be transported around the bend. Fast moving molecules are lost from the guide and the quadrupole bend therefore acts as a low-pass velocity filter to produce a continuous beam of molecules with a low translational temperature.

The transmission of molecules through the guide depends on the high voltage applied to the quadrupole, the radius of the bend and the Stark-shift to mass ratio of the molecular quantum states. Figure 5(b) shows velocity distributions, measured in our laboratory, for $ND_3$ molecules emitted from an electrostatic quadrupole guide with a bend radius of 12.5 mm, operating at different quadrupole voltages. The lack of molecules with velocities below 20 $ms^{-1}$ is believed to arise from the acceleration caused by the fringe fields at the end of the guide [129]. Typically, around $10^8$ molecules $s^{-1}$ can be produced as a continuous flux at the exit of the quadrupole [128]. As the molecules are loaded into the quadrupole from an effusive source, the guided molecules are produced in a wider range of rotational quantum states compared with molecular beam deceleration techniques. Some state purification is possible as a consequence of the different Stark shifts of the rotational levels; the rotational distribution of formaldehyde molecules exiting such a guide was recently measured in a depletion spectroscopy experiment in which the tunable narrow-bandwidth UV radiation from a continuous ring dye laser was used to state-selectively photodissociate molecules within the quadrupole guide [130].

This source of cold molecules has several potential advantages for use in studies of low energy chemical reactions. Firstly, the molecules are produced as a continuous flux, and therefore the possibility exists to accumulate significant numbers of cold molecules in an electrostatic trap [131]. Secondly, the source is relatively simple to operate and is compact, in comparison with the Meijer-type Stark decelerator. Thirdly, the application of a radiofrequency oscillating field to the quadrupole allows "high-field seeking" molecules to be guided and this feature enables application to heavy molecules. For example, a related type of experiment using the neutral-molecule analogue of a quadrupole mass filter has shown that it is possible to spatially separate two conformers of 3-aminophenol in a molecular beam [132].

One disadvantage is that although the translational temperature of the selected beam gets lower as the quadrupole voltage is reduced, the number density of molecules will also be substantially reduced. Thus in practical terms it may be difficult to achieve useful densities of molecules with translational temperatures much lower than ~500 mK, unless one starts with a cooled effusive source. Nevertheless, starting with a room temperature source of methyl fluoride molecules, low-energy studies of the chemical reaction $CH_3F + Ca^+ \rightarrow CH_3 + CaF^+$ have recently been carried out in Oxford [35] (see Section VI).

The relatively low fluxes of molecules that can be produced from the quadrupole guide simply reflects the low number of slowly moving molecules in the effusive source distribution; higher fluxes can be achieved by cooling the nozzle. At low temperatures this approach is limited by condensation of the gas inside the nozzle, but it has recently been shown that the effusive source can be surrounded by a cryogenic environment of helium buffer gas

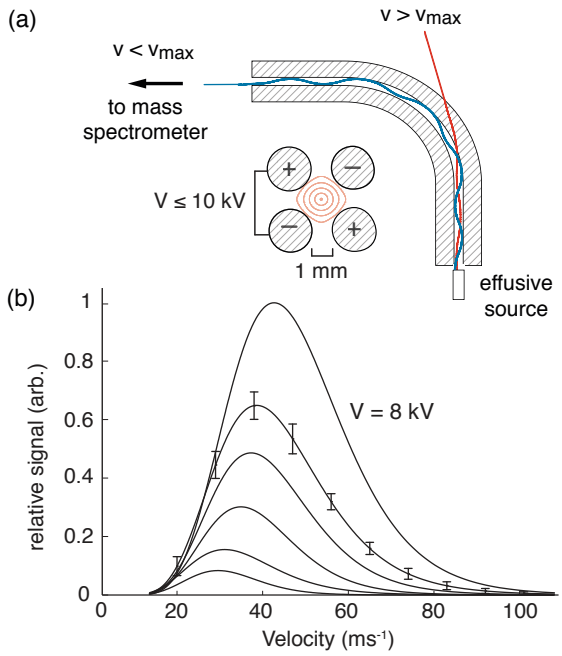


FIG. 5: (a) Velocity selection using a bent electrostatic quadrupole guide. (b) Experimental velocity distributions of velocity-selected beams of $ND_3$ molecules with different potential differences applied to the quadrupole electrodes (1 kV increments, starting from 3 kV for the lowest intensity beam). The measurements were obtained by pulsing the high-voltage applied to the quadrupole and recording the arrival times of molecules at the mass spectrometer.

[133, 134]. By tuning the density of helium atoms near the nozzle exit, it is possible to cool the translational degrees of freedom of the molecules, better matching the emittence of the effusive beam to the acceptance of the guide. Furthermore, the buffer gas density allows the rotational state populations to be tuned to produce beams with higher quantum state purities. Using a helium density of $10^{14}$ $cm^{-3}$, van Buuren *et al.* [135] obtained a guided flux of around $7\times10^{10}$ $ND_3$ molecules $s^{-1}$ with a measured average velocity of 65 $ms^{-1}$. Formaldehyde molecules were also guided using this source and it was found that 82% of the transmitted population was in a single rotational quantum state [135].

Finally, in a different approach, Arndt and co-workers have also shown that beams of slowly-moving heavy (< 6000 a.m.u.) molecules can be produced using a series of helical grooves milled into a rotating metal cylinder to create a mechanical velocity selector [136].

### C. Cold atom methods

A different "synthetic" route to produce cold molecules starts from the fairly dense, ultracold ensembles of atomic alkali atoms that can be produced through laser cooling. By pairing cold atoms together, diatomic molecules can be produced in two different ways: through photoassociation or magnetic Feshbach resonance tuning [137]. In both cases, the very low collision energy limits the total angular momentum and so the molecules are typically produced with little rotational excitation. The formation of the molecules at large separations, however, leads to highly excited vibrational states and there has been significant ef-

fort aimed at removing this excitation. From a chemical perspective, molecules created this way are particularly unusual, with a de Broglie wavelength significantly larger than typical molecular dimensions. In certain cases, these molecules can be produced with sufficiently high phase space densities to allow Bose-Einstein condensation and, using fermionic atoms such as $^6$Li and $^{40}$K, these molecular BECs have been used to investigate the formation of the composite-Boson "Cooper pairs" that feature in the BCS theory of superconductivity [138, 139].

#### 1. Photoassociation

The photoassociation technique [140] starts with laser-cooled atoms and uses laser-induced association to generate electronically excited (and highly vibrationally excited) dimer species. The technique has been applied to form dimers of alkali or alkaline earth metals and heteronuclear species with two different alkali dimers *e.g.*, RbCs [141]. As shown in Fig. 6(a), the long-range attractive potential between two atoms changes the excitation energy of the atom when it is in the presence of a second atom – typically, for alkali metal interactions, the depth of the interaction between an excited atom and a ground state atom is stronger than between two ground state atoms. Thus, if the atoms are irradiated continuously with light at a frequency just below the excitation frequency of the atom, and the kinetic energy of the atoms is negligible (which is a good assumption for laser-cooled atoms) then at a certain separation there will be a transition between the unbound ground state pair of atoms and a very high vibrational level of the excited state of the dimer, as shown in Fig. 6(a). Consequently photo-induced dimerization occurs, and by scanning the laser frequency, a series of spectroscopic transitions is observable, each corresponding to the production of different vibration-rotation levels of the bound molecule. However, in order to get the molecules into the electronic ground state and to reduce the degree of vibrational excitation, further laser-induced (*e.g.*, using shaped femtosecond pulses [142]) or spontaneous transitions are required. Some recent progress in this direction is summarised in Section IIIC.3 below.

#### 2. Feshbach resonance magnetic tuning

A Feshbach resonance is a scattering resonance which occurs when the collision energy of the two colliding atoms becomes degenerate with a bound level of an excited state of the diatomic molecule. At such energies there may be an enhancement of scattering cross sections, and a dramatic change in the scattering length (see Section VI), as a result of the colliding atoms becoming transiently captured into a bound state of the dimer (see Ref. [144]). The general situation is illustrated in Fig. 6(b). In practice this technique starts with laser-cooled alkali metal atoms and the energies of the colliding pair are extremely low. The bound state is a highly vibrationally-excited state of the dimer potential which typically correlates with a different hyperfine state of one of the two atoms. As the hyperfine states have different magnetic moments, bound-states can be brought into resonance with the energy of the colliding atoms by applying an external magnetic field. Consequently, Feshbach resonances can occur at specific magnetic field strengths; in Fig. 6(b) these fields essentially correspond to the point where the molecular resonance crosses zero energy. Sweeping the field through this value allows the system to be transformed smoothly from atoms to molecules, in some cases with near 100% efficiency. Experimentally, the existence of molecules can be clearly shown in a Stern-Gerlach type experiment in which the alkali-metal dimers are separated from the unconverted atoms using a magnetic field gradient. The molecules are subsequently dissociated by applying a reverse-sweep of the magnetic field to allow imaging of the released atoms. This is illustrated by the atomic absorption image shown in Fig. 6(b), obtained by Rempe and co-workers [143], in which two spatially-separated Rb atom clouds were produced: the left arising from unconverted atoms, the right from dissociated molecules.

Though highly excited, Feshbach molecules are produced in specific rovibronic states which can be manipulated (to a limited extent) using radiofrequency magnetic fields [145]; used to investigate universal few-body physics in so-called "Halo states" [146], or three-body Efimov states [147]; and used for the production of molecular BECs [139, 148]. Indications of scattering resonances in a $Cs_2$ molecular gas [149], as well as the observation of collisions with Cs atoms (see Section V), suggest that it may also be possible to form alkali-metal trimers or even tetramers through magnetic-field tuning. Molecules formed via controlled collisions of ultracold atoms retain the quantum mechanical coherence that existed in the original ultracold atomic gas, suggesting that many-body effects or "superchemistry" might also be observable [22–24].

#### 3. Transferring population to the vibrational ground state

For both Feshbach-resonance tuning and photoassociation, translationally ultracold molecules are formed in vibrationally excited states near the dissociation limit. Considerable efforts have been directed at devising schemes for transferring population to the ground state, with much recent success. DeMille and co-workers have shown that RbCs dimers formed by photoassociation decay primarily by fluorescence to the $\nu = 37$ state of the $a^3\Sigma^+$ electronic state. These molecules can then be transferred to $\nu = 0$ of the $X^1\Sigma^+$ state via a stimulated emission pumping process, *i.e.*, laser excitation of the molecules into a more highly excited state followed by a down-pumping step by a second laser. A detectable quantity of ground state ($\nu = 0$) dimers can be formed this way [141]. In the case of LiCs, Weidemüller and co-workers [150] have found that photoassociation to the $B^1\Pi$ state can populate levels as low as $\nu' = 4$ which then have a high probability of spontaneous fluorescence to the $\nu'' = 0, J'' = 0$ and 2 levels of the ground state at a temperature of 260 $\mu$K. The production rate in these experiments is equal to $5 \times 10^3$ molecules s$^{-1}$, and the advantage in this case is that no extra lasers are required to transfer the population to the ground state. Pillet and co-workers have shown [151] that a pulse from broadband femtosecond laser can be used to drive transitions between the relatively low-lying ground state levels $\nu = 0$–10 that are formed by spontaneous emission from the $B^1\Pi_u$ state of $Cs_2$ following photoassociation. Using optical pulse shaping the population transfer to $\nu = 0$ can be optimized to give over 70% population transfer and the method is expected to be broadly appli-

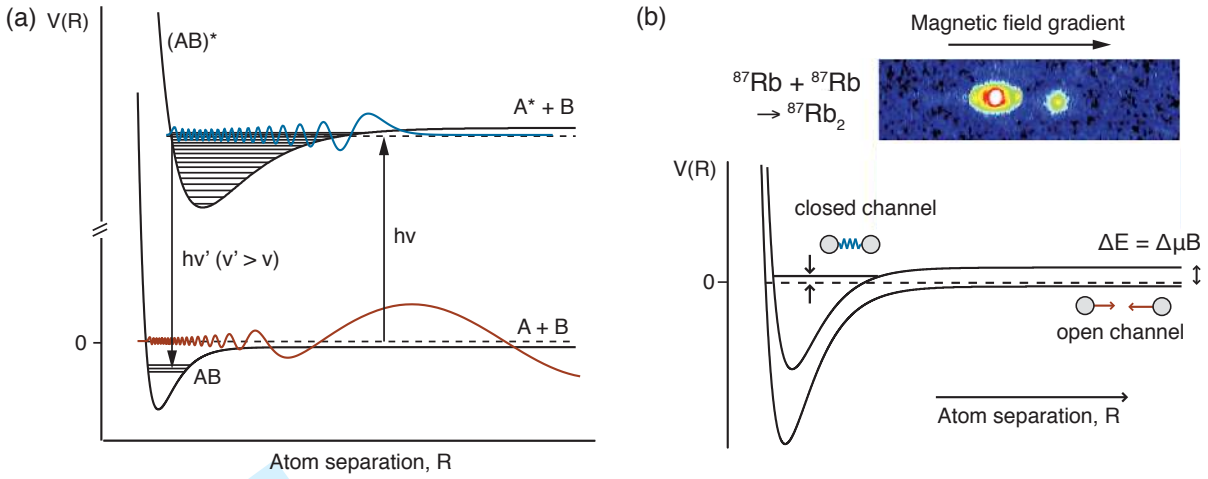


FIG. 6: (a) Photoassociation of laser-cooled atoms. Illumination of an ultracold atomic gas with a laser tuned to slightly below the atomic excitation frequency allows a pair of colliding atoms to absorb a photon. This absorption forms a vibronically excited dimer state which can then decay either by stimulated or spontaneous emission to bound states of the ground electronic potential. (b) Feshbach resonance magnetic tuning. The energy difference of two potential energy curves which correlate with different hyperfine states of the colliding atoms can be tuned using external magnetic fields. At certain field strength the colliding atoms are converted to molecules. The inset shows an absorption image of two Rb atomic clouds produced by separating and then dissociating the molecules (right) from the original atom cloud (left). Experimental results adapted from Ref. [143].

cable. Lang *et al.* have used a stimulated Raman process (STIRAP) to transfer nearly 90% of the population from the $\nu = 36$ level in the deeply bound $a^3\Sigma_u^+$ state of $Rb_2$ into its $\nu = 0$ ground state via the excited $^3\Sigma_g^+$ surface [152]. The population transfer was performed in a 3D optical lattice which allowed the ground state molecules to be trapped. Similarly Ye and co-workers have used STIRAP to transfer population of KRb polar molecules to the ground vibrational level of the lowest triplet state and have stated that a density of $10^{12}$ cm$^{-3}$ ($3 \times 10^4$ molecules in an optical dipole trap) and a translational temperature of 350 nK [153]. The significance of these developments is the likelihood that BECs or Fermi-degenerate gases could be achievable with these homonuclear and dipolar ground-state dimers in the near future.

### D. Collision-based methods

#### 1. *Buffer-gas cooling*

Perhaps the most natural way of cooling molecules is to simply immerse them in a very low temperature bath of buffer gas and then rely on elastic collisions to dissipate the excess molecular energy. Such an approach has been pioneered by Doyle and co-workers [154] and has also been implemented by Bakker *et al* [155]. Though simple in principle [156], there are a number of challenges associated with these experiments [157]. The molecules must avoid interacting with the cryogenically cooled walls of the gas chamber where they would be adsorbed, and there must be a means to retain and isolate the cold molecules when the buffer gas is pumped away. This requires the use of large inhomogeneous magnetic fields to trap molecules in low-field seeking Zeeman states in the centre of the chamber. As such, this technique can only be applied to molecules with a sufficiently large magnetic dipole moment. To date, magnetic trapping has been demonstrated for CaH, NH and VO [154, 158, 159], and more recently for CrH ($X^6\Sigma^+$) and MnH ($X^7\Sigma^+$) [160], as well as numerous atoms [161–164].

The molecules (or atoms) to be cooled can be formed by laser ablation or loaded into the gas cell from a molecular beam. Crucially, the molecules must thermalize to the temperature of the buffer gas ($T < 4$ K) and relax into the conservative magnetic trapping potential before they reach the walls of the gas chamber. As this typically requires several hundred collisions, a high buffer gas density of around $10^{16}$ cm $^{-3}$ is needed. To achieve the lowest temperatures, helium gas is used as it still has an appreciable vapour pressure even down to a temperature of only a few hundred mK. However, subsequent removal of the helium, either by cryopumping or through a large-aperture cryogenic valve, is necessary to prevent molecules being lost through thermal evaporation from the trap or through Zeeman relaxation. Figure 7 shows a schematic representation of the experimental setup for trapping NH molecules. The trap lifetime of the NH molecules depends on the density of He atoms in the trapping chamber and at high densities the molecules are lost through Zeeman-state changing collisions.

Once isolated from the buffer gas, the trapped species continue colliding with one another to form a new thermal distribution which may provide the starting point for evaporative cooling [165]. In principle high densities of trapped molecules may be obtained, potentially allowing studies of low-temperature collisions such as those already performed with trapped cold atoms such as Mn [166] and Cr [167].

In an interesting development, Patterson and Doyle have also used buffer-gas cooled atoms and molecules as a source for a magnetic octopole guide [133] (analogous to the electric quadrupole velocity selector described above), allowing the production of a high-intensity cold beam source of $O_2$ molecules with a guided flux of around $10^{12}$ molecules s$^{-1}$. In this device, the molecules effuse through a two-stage cell filed with helium gas and are emitted with velocities similar to the cold helium (about 60 ms$^{-1}$) so that the effective temperature of the molecules is of order 10 K or more. The relatively high fluxes obtained

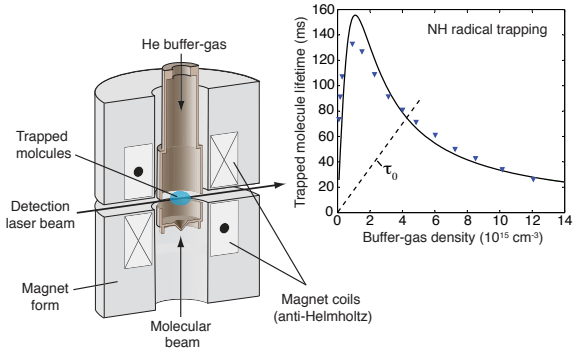


FIG. 7: Buffer-gas cooling. Left: Schematic representation of the experimental apparatus for trapping NH radicals. Right: Lifetimes of trapped NH molecules as a function of the buffer-gas density (adapted from Ref. [159]).

and expected low rotational temperature suggest this type of source may be useful for collision studies or trapping experiments.

### 2. *Superfluid helium droplets*

Although helium droplets represent a rather different source of cold molecules, we mention them briefly for completion. Helium droplets are formed by expansion of a high pressure of cryogenically cooled He at a pressure of order 20 bar. Typical helium clusters have sizes ranging from $10^3$ to $10^8$ atoms [168]. One of the most important developments has been the demonstration that helium droplets passing through a gas cell may pick up one or more molecules as they are transmitted [169]. Secondly it has been discovered that, because the helium droplet is superfluid, the molecules can rotate and vibrate almost freely and therefore spectroscopic measurements may produce sharp rotational lines [170], similar to gas phase spectra. Molecules in helium droplets have also been photoionized [171]. Typically the absorption of light leads to energy transfer that ultimately leads to a reduction in the number of molecules in the droplets. Thus the absorption can be detected by monitoring the mass change. The molecules formed in helium droplets may be located on the surface or in the centre of the droplet. If two molecules, or two atoms, are collocated in a single droplet then the possibility exists for reaction to occur between them. Such reactions are likely to have a different behaviour from reactions in the gas phase because of the existence of the weakly interacting energy sink (the helium droplet). Toennies and co-workers studied ion-molecule reactions within helium droplets [172]. $He^+$ ions formed inside the droplets by electron impact ionization were allowed to react with $D_2$, $N_2$ or $CH_4$. Charge transfer reactions occurred at a temperature of 0.38 K and secondary reactions of the primary product ions were also observed to occur (*e.g.*, secondary reactions of $CH_4^+$ with $D_2$.) Transient intermediate species such as $CH_3D_2^+$ could be stabilized within the clusters in certain cases. Reactions between barium atoms and $N_2O$ molecules were also studied within helium droplets by observing the chemiluminescence of the BaO product molecules [173].

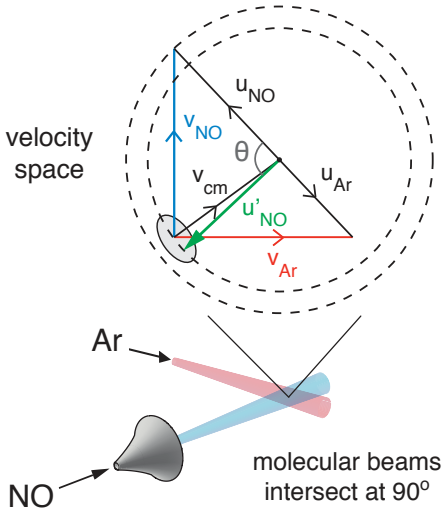


FIG. 8: Newton diagram for single collision cooling. Molecular beams of NO and Ar intersect at right angles and scatter over a wide range of angles. A small fraction of NO ($^2\Pi_{1/2}$, $j$ = 1/2) molecules are inelastically scattered through angles close to $\theta$, into the $^2\Pi_{1/2}$, $j'$ = 15/2 rotational state. For these molecules, the centre-of-mass frame velocity cancels the laboratory frame velocity, producing a stationary distribution (shaded area). The dashed circles represent the limiting the centre-of-mass frame recoil velocities for elastically scattered (outer) and inelastically scattered (inner) NO molecules.

### 3. *Kinematic cooling using inelastic and reactive collision*

Single "billiard-like" collisions in crossed supersonic molecular beams can be used to produce molecules that are stationary in the lab frame. For example, Chandler and co-workers [174, 175] have used velocity-mapped ion imaging methods to demonstrate the production of slowly moving NO molecules in a crossed-beam scattering experiment with Ar atoms. As is shown in the Newton scattering diagram in Fig. 8, the technique relies on the vector cancellation between the recoil velocity of the NO molecules $\mathbf{u}'_{\rm NO}$ and the centre-of-mass velocity of the collision partners $\mathbf{v}_{\rm cm}$,

$$\mathbf{v}'_{\rm NO} = \mathbf{v}_{\rm cm} + \mathbf{u}'_{\rm NO} \approx 0. \qquad (9)$$

As the molecules must be scattered in both the right direction (opposite to $\mathbf{v}_{\rm cm}$) and with the correct speed, this cancellation occurs for only a small fraction of the molecules in the beam. Nevertheless, NO molecules with final velocities less than 15 $\rm ms^{-1}$ can be generated in a single quantum state at densities approaching $10^8$ molecules $\rm cm^{-3}$ [175]. If the collision partners have non-identical masses, momentum constraints mean that very low final velocities can only be achieved if a specific amount of excess translational energy can be accommodated in the internal modes of the molecule. For beams intersecting at right angles, the necessary change in the internal energy of the molecule is given by:

$$\Delta E_{\rm int} = \left(1 - \frac{m_a}{m_b}\right) E_a, \qquad (10)$$

where $m_a$ and $E_a$ are respectively the mass and initial lab frame kinetic energy of the molecule to be cooled and $m_b$ is the mass of the atomic collision partner. In the experiments of Chandler and co-workers, this excess energy was taken up by rotation

of the NO molecule through the inelastic transition NO ($^2\Pi_{1/2}$, $j$ = 1/2) → NO ($^2\Pi_{1/2}$, $j'$ = 15/2). Although most NO molecules are scattered into different quantum states, those remaining with very low velocities are produced in only a single rovibrational state.

Further analysis of the scattering kinematics [46, 174] predicts that the post-collision velocity distribution of the NO molecules should be significantly narrowed. This "kinematic compression" arises because the centre-of-mass and recoil velocities scale similarly with small changes in the velocity of the NO molecules and cooling to translational temperatures below the ∼400 mK that was measured in the initial experiments should be possible. Intersecting the molecular beams in the centre of an electrostatic or magnetic trap, or using laser-cooled atoms as the collision partner may potentially allow confinement of the stopped molecules.

This type of collisional cooling is not limited to purely inelastic collisions. Liu and Loesch [176] have shown that slow molecules can also be generated by reactive collisions. Using counter-propagating beams of HBr and K atoms, KBr molecules with speeds below ∼60 ms$^{-1}$ were produced from the chemical reaction K + HBr → KBr + H. These experiments rely on the very small mass ratio, $m_{\rm H}/m_{\rm KBr}$, and careful tuning of the reactant beam velocities to ensure that the maximum centre-of-mass frame recoil velocity of the KBr molecules is very small. Notably high intensities ($> 10^{11}$ molecules s$^{-1}$ sr$^{-1}$) of slow KBr molecules can be produced this way. A general analysis for producing cold molecules from reactive collisions has been given [46].

A novel variant on these collision-based methods, which remains to be demonstrated, is to photodissociate molecules in a molecular beam in such a way that the fragments are ejected backwards along the beam direction to cancel the velocity of the parent molecule. This requires finding a photodissociation process that produces fragments with a low, well-defined energy, together with a highly directed angular distribution. One possible system would be $NO_2$ for which there is strong absorption close to the dissociation threshold, a tuneable photofragment energy and a strongly polarised angular distribution of the photofragments [177].

## IV. TRAPPING AND SECONDARY COOLING TECHNIQUES

### A. Trapping cold and ultracold molecules

A variety of potential applications of cold molecule sources would benefit from, or absolutely require, the trapping and storage of cold and ultracold molecules on a timescale from milliseconds to hours. Such long timescales for observation could provide collisional experiments with increased sensitivity, and would eliminate transit-time broadening as a limiting factor in ultra-high resolution spectroscopy. The secondary cooling of cold-molecules produced in the millikelvin temperature range into the ultracold regime, via evaporative, sympathetic, or cavity cooling methods (see section IVB) would also require long storage times. A number of traps have been designed for neutral molecules making use of inhomogeneous magnetic, electric or optical fields and these developments are briefly reviewed in this section.

#### 1. *Electrostatic traps*

Polar molecules that have been decelerated in low-field seeking states can be trapped using static inhomogeneous electric fields. This was first demonstrated by Bethlem and co-workers who applied high voltages to the electrodes of a quadrupole trap consisting of a ring electrode with two endcaps [74] to create a deep electric field minimum in which Stark-decelerated $ND_3$ molecules could be confined at a translational temperature of 25 mK. The trap was mounted at the end of the Stark decelerator and loaded by switching the high voltage applied to the endcap electrodes so that a decelerated beam moving at around 15 ms$^{-1}$ could be admitted whilst simultaneously undergoing a final deceleration step to bring the molecules to a standstill in the trap centre. Several molecular radicals such as OH and NH (and also metastable CO) have been trapped using this method. Trap lifetimes greater than ∼1 s have allowed the effects of optical pumping by blackbody radiation to be observed [87] and direct measurements to be made of the radiative decay lifetimes for vibrationally excited or metastable molecules [72, 73]. Evolutionary strategies have also been implemented to improve the efficiency of the loading process [178].

Veldhoven *et al.* have reported the implementation of a more versatile 4-electrode electrostatic trap [179], shown in Fig. 9(a), that is capable of creating dipolar, quadrupolar or hexapolar fields. By superposing the dipolar and hexapolar fields, a double-well or single-well potential can be generated and the trap can be rapidly switched between the different field configurations. As the double well potential allows two packets of molecules to be stored on either side of a barrier (as has been demonstrated for $^{15}ND_3$ [179]), the different field configurations might be used in future experiments with more dense samples to produce collisions between packets of trapped molecules.

Electrostatic trapping has also been demonstrated with methods other than Stark deceleration. Kleinert and coworkers have realized a thin wire electrostatic trap consisting of four concentric rings and used it to trap ultracold NaCs molecules formed by photoassociation of cold atoms to $\nu$ = 19–25 in an Magneto-Optical Trap (MOT) [180]. The electrostatic trap is designed so that it can be superimposed on the MOT and, given the low temperature of the molecules (∼200 $\mu$K), the electrostatic fields required for trapping are relatively low. A trapping lifetime of 225 ms was found, limited by the background pressure. Rieger *et al.* have reported a "leaky" electrostatic trap formed from a series of ring and cap electrodes [131] into which velocity selected $ND_3$ molecules from a bent quadrupole guide can be continuously loaded, achieving a lifetime of 130 ms for molecules in the trap at a density of $10^8$ cm$^{-3}$ and a temperature of 300 mK.

#### 2. *AC electric traps*

Electrostatic traps have the advantage of being deep (∼1 K) and relatively large volume (∼0.1 cm$^3$), but they can only be used to confine molecules in low-field seeking quantum states. The trapping of molecules in high-field seeking states is of potentially greater importance as the lowest energy states of all molecules, and the majority of states for large molecules, are high-field seeking in character. Sympathetic or evaporative cooling through elastic

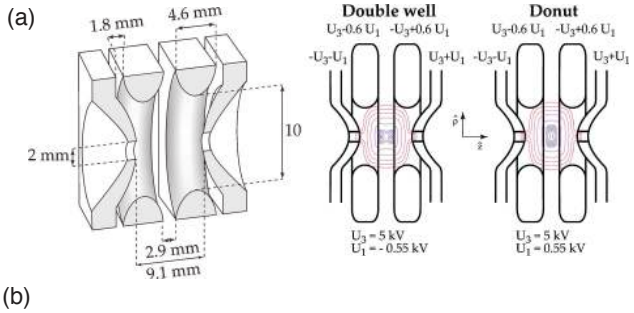


FIG. 9: Electric trapping of polar molecules. (a) Electrostatic trap for confining low-field seeking molecules in various trapping geometries. (b) Linear AC trap for high-field and low-field molecules, showing the two electric field configurations used for electrodynamic trapping. Adapted from Refs. [78, 179].

collisions (see Section IVB1) is also only likely to be successful for molecules in their ground states; higher energy states will incur inelastic collisions leading to heating or trap loss. Maxwell's equations do not allow the possibility of creating a field maximum in free space in which to trap high-field seeking molecules, hence a different approach is required using alternating fields [77, 91] or a geometry in which the molecules perform circular motion around an electrode [181]. For AC trapping, several different electrode geometries have been tested experimentally based on the Paul trap, linear Paul trap and three-phase traps developed for charged-particles [77]. Radio-frequency voltages are applied to the trap electrodes to create an oscillating electric field saddle-point in the trap centre: at a given instant, the trapped molecules experience a force away from the centre of the trap in at least one dimension, and forces towards the centre in the others. The periodic focusing and defocusing caused by the oscillating electric fields allows dynamic confinement of both high-field and low-field seeking molecules (the saddle point effectively rotates around to create a time-averaged effective potential which confines molecules near the centre of the trap).

The linear AC trap designed by Schnell *et al.* [78], shown in Fig. 9(b), consisting of four 8 mm length double rods, has been used to capture $^{15}ND_3$ molecules which were decelerated to 15 $ms^{-1}$ before trapping. The deceleration was carried out on low-field seeking states and these were driven into high-field seeking states using a microwave pulse. The first pair of electrodes is used as a final deceleration stage before switching to the trapping potentials, allowing efficient loading of the trap. The trap depth is much less for AC traps than for the electrostatic versions: the depth was found to be around 10 mK in this case and the molecules were confined to a volume of less than $10^{-3}$ $cm^3$. An alternative design of AC trap, with a cylindrically symmetric electrode geometry, is estimated to have a 5-times better acceptance than the linear quadrupole trap but inferior access for detection laser beams and for superimposition of ultracold atom samples for sympathetic cooling [77].

Ground state atoms can also be trapped in AC traps as a result of the induced dipole moment and the second-order Stark interaction. Schlunk *et al.* demonstrated the trapping of $^{87}Rb$ atoms transferred from an MOT in a cylindrically symmetric AC trap with two ring-electrodes and two hemispherical electrodes [182, 183]. Around $10^5$ atoms were trapped at 100 $\mu$K. Ideally one might aim to simultaneously trap molecules and atoms in such a trap, but unfortunately polarisable atoms and molecules cannot generally be trapped at the same frequencies. Nevertheless it was demonstrated in this work that a magnetic trapping field could be superimposed on the electric trap and the Rb atoms remained trapped at AC electric fields that in principle could be used for trapping polar molecules (see below). Rieger *et al.* developed a three-phase AC trap for Rb atoms at 70 $\mu$K [184] and proposed that the frequencies and amplitudes employed should be appropriate for storing the $H_2O$ or $D_2O$ molecules; the polarizability-to-mass ratio is critical in the context of trapping very different types of atom/molecule simultaneously.

### 3. *Optical and microwave traps*

Molecules can also be trapped by intense optical fields [185, 186]. As in the case of the optical decelerator (Section IIIA4) the attraction of the molecules to the focal point of the laser field depends on the polarizability of the molecules rather than the sign of the Stark shift. Using a 110 W $CO_2$ laser focused to a beam waist of around 80 $\mu$m, Zahzam *et al.* produced a trap depth of order 1 mK for $CS_2$ molecules [187]. DeMille *et al.* also demonstrated optical trapping of RbCs molecules in their metastable $^3\Sigma^+$ state and studied the inelastic collisions of the trapped atoms [188]. An extension of this method is to produce an optical lattice by superposition of laser beams and to then trap individual molecules on each high-intensity antinode of the lattice [2]. In experiments where ultracold molecules are formed by photoassociation or Feshbach Resonance tuning, the ideal approach is to first trap ultracold atoms in the lattice and then to bind them together into molecules using the methods described previously. Three-dimensional lattices of ultracold $Rb_2$ molecules have been prepared this way [189], with some control over the internal and external states [190], and it has even been possible to generate molecules from an atomic Mott-insulator state so that one molecule per lattice site is formed [191]. Similar lattice trapping experiments have been performed using KRb molecules [153, 192].

A related development is the proposal for a microwave trap in which molecules are trapped in the free-space standing-wave maximum of a resonant microwave cavity [193]. The principle is based on the AC Stark shift. For example, if the circularly polarised microwave radiation is red-detuned with respect to the $J = 0 \rightarrow 1$ rotational transition then the $J = 0$ molecules become attracted to the maximum of the field. Such a device has yet to be demonstrated, but it is expected that large trap depths ($\geq$ 500 mK for a dipole moment of 1 D) could be achieved, with large acceptance volumes (several $cm^3$), which should be well-suited for loading using a Stark decelerator.

### 4. *Magnetic and magneto-optical trapping*

Magnetic trapping forms the basis for the buffer-gas cooling technique described in Section IIID , which has

been used to prepare CaH, NH, VO, CrH and MnH molecules at temperatures of a few hundred mK. Atoms or molecules slowed using a Zeeman decelerator may also be loaded into a magnetic trap (as has been demonstrated with H atoms [103]). The advantages of employing a magnetic trap include the possibility of simultaneously trapping ultracold atomic gases with ultracold molecules providing opportunities for sympathetic cooling [194]. In addition, the use of a magnetic trap instead of an electrostatic trap allows the application of a separate independently controllable electric field, which might be used to modify the collision dynamics [12]. Ye and co-workers have succeeded in magnetically trapping the slow beam of OH molecules from a Stark decelerator, using a pair of coils in anti-Helmholtz configuration [79]. The molecules were trapped at a density of 3 $\times 10^3$ cm$^{-3}$ with a well-depth of 30 mK. These authors also demonstrated that the trap could be surrounded by an electric quadrupole to apply an independent electric field. Permanent magnets have also be used to reflect [81] or trap [195] Stark-decelerated OH molecules. Alkali metal dimers have been trapped in the quadrupolar magnetic field present in a MOT [196, 197]. For example, KRb molecules in a high vibrational level of their lowest triplet state were magnetically trapped at a temperature of around 300 $\mu$K by Wang *et al.* [197] following photoassociation in a dual species K/Rb MOT.

Ye and co-workers have recently proposed the development of a magneto-optical trap for polar molecules [61]. Taking TiO as an example they point out that for a molecule where the lowest rotational level of an electronically excited state is $J = 0$ and the lowest rotational level of the ground state is $J = 1$ (in this case because the symmetry is $^3\Delta_1$), laser cooling might be possible because the spontaneous fluorescence from the excited state can only occur to the $J = 1$ level; thus, the absorption and emission cycle is relatively closed. The fluorescence will nevertheless be spread over transitions to several vibrational levels and one repumping laser would be required for every possible excited vibrational level accessible. In the case of TiO the Franck Condon factors favour only small changes in vibrational quantum number and the number of such repumping lasers required could be as few as two. The use of a magneto-optical trap in conjunction with this laser cooling process could be accomplished, provided a pulsed electric field is used to non-adiabatically mix the ground state magnetic levels to ensure interaction with the cooling lasers [61]. Again, this scheme has not yet been demonstrated experimentally.

### 5. *Trapping ions*

The challenge of trapping cold molecular ions is closely related to the problem of trapping high-field seeking neutral molecules. For positively-charged particles, stable confinement requires a restoring force, $\nabla \cdot \mathbf{F} < 0$, about a local minimum of the electrostatic potential, but this cannot be achieved in charge-free space as the Laplace equation, $\nabla^2\phi = 0$, permits only saddle-like stationary points. Trapping of atomic and molecular ions is possible, however, using oscillating potentials and the technology to trap ions using radiofrequency fields is well-established and has been reviewed extensively [198, 199]. Ions in a radiofrequency trap exhibit two forms of motion; a long-range, low-frequency secular motion, which is determined by the time-averaged effective potential, and a short-range higher frequency micromotion, which follows the rapidly oscillating radiofrequency fields. Although a secular temperature of the ions is often quoted for ions in traps, which ignores the effects of micromotion, the use of ion traps in collisional experiments requires the full motion to be considered [198].

The two most common traps currently employed in cold ion experiments are either quadrupole traps (Paul traps) which have been established for over fifty years, or the 22-pole trap designed more recently by Gerlich *et al.* [200]. As the number of alternating polarity electrodes increases, the effective potential becomes flatter in the centre of the trap and ions moving away from the trap axis are less susceptible to the micromotion of the radiofrequency field (and hence are colder and more stable in the presence of collisions with a buffer gas). A growing number of applications are being developed in which molecular ions are cooled using He buffer gas to a few Kelvin in a 22-pole trap so that spectroscopic or collision experiments can be performed. For quite large molecular ions of biological interest it has been shown that very high resolution spectra can be obtained [201]. Through equilibration with the helium buffer gas, the ions are internally cold as well as translationally cold. Anions have also been cooled and trapped in such devices [202] and applied in collision studies [203].

Certain atomic ions, most commonly the singly-charged alkaline earth ions $Be^+$, $Mg^+$ and $Ca^+$ and $Ba^+$, can be laser cooled in an ion trap (usually a quadrupole trap as this gives best access for the cooling laser beams.) As the temperature is lowered into the millikelvin range a phase transition may occur to produce "Coulomb crystals" (or clusters) in which ordered structures of ions are observed, with a typical ion spacing of 20 $\mu$m [199] (see Fig. 10). According to the number of ions trapped and the field amplitudes applied, the crystals may be one-dimensional strings or two/three-dimensional structures. The ions are detected through their fluorescence induced by the cooling laser which continuously irradiates them throughout the experiment. A microscope objective lens can be used in conjunction with a CCD camera to observe a two-dimensional projection of the crystal. Individual ions are easily observable, the spot size on the image being determined by the ionic motion (although in fact molecular dynamics simulations indicate that the ions can diffuse through the crystal on a time-scale which is not normally resolved). The effective temperature near to the axis of a Paul trap is of order 10 mK, while the micromotion increases in the outer layers of the Coulomb crystal.

One of the most important properties of a Coulomb crystal is the facile sympathetic cooling of molecular ions which are generated within the trap (*e.g.*, by photoionization, electron impact or chemical reaction) [204]. The strong Coulomb forces between ions ensure that there is effective transfer of kinetic energy out of the system via the continuous laser cooling process. The sympathetically-cooled molecular ions do not fluoresce but they can have a pronounced influence on the shape of the observed shells of atomic ions. The mass dependence of the effective trapping potential means that lighter ions are located closer to the trap axis. In Fig. 10(a) this can be seen from the fluorescence produced by laser-cooled $^{24}Mg^+$ ions in a $^{40}Ca^+$ Coulomb crystal, whilst in Fig. 10(b) sympathetically-cooled $H_3^+$ ions produce a dark core within the $^9Be^+$ Coulomb crystal. Mass spectrometric methods can also be used to monitor the presence of molecular ions in the trap [199]. The sympathetic cooling of molecular ions

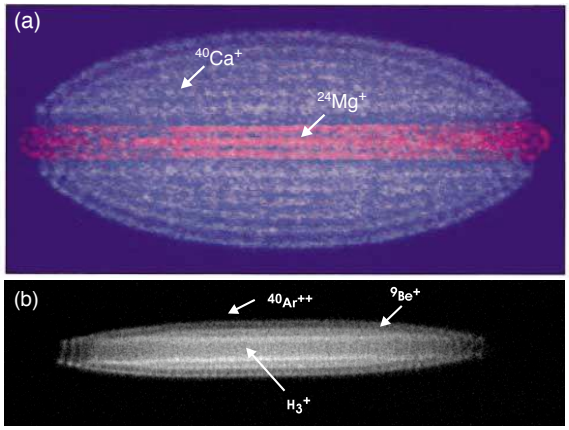


FIG. 10: Coulomb crystals (a) Image of a bicomponent crystal in which the fluorescence produced by laser cooling $^{24}Mg^+$ and $^{40}Ca^+$ ions is simultaneously observed (adapted from Hornekaer *et al.* [210]). (b) Fluorescence image of a $^{9}Be^+$ Coulomb crystal containing sympathetically cooled $H_3^+$ and $^{40}Ca^+$ ions (adapted from Roth *et al.* [211])

provides a versatile means to produce translationally cold molecules, but in general the internal degrees of freedom are not equilibrated [205]; inelastic collisions between ions typically do not occur because the Coulomb force prevents the close approach of the ions, and thus the vibration-rotation temperature of the ions is that of the environment, typically room temperature. Spectroscopic pumping schemes have been proposed to achieve internal cooling of trapped molecular ions [206–209].

### B. Secondary Cooling

With the exception of the techniques involving ultracold atoms, the methods discussed so far produce molecules at characteristic translational temperatures greater than several millikelvin. In order to bridge the gap between currently achievable temperatures and the ultracold limit, secondary methods to further cool trapped molecules are therefore needed. In contrast to the schemes designed to transfer rovibrationally excited molecules to their ground states, in this section we concentrate on three emerging techniques which might be used to provide higher phase-space densities of trapped molecules.

#### 1. *Sympathetic cooling*

As discussed above, ensembles of trapped molecular ions can be efficiently cooled to millikelvin temperatures through their long-range Coulomb interaction with laser-cooled atomic ions, while elastic collisions between neutral molecules and a helium buffer gas allow cooling to around 1 K. Similarly, trapped cold molecules might potentially be brought into the ultracold regime by placing them in thermal contact with a gas of ultracold atoms. This type of sympathetic cooling has already been demonstrated in binary mixtures of laser-cooled atoms with different spin states [212], isotopic masses [213] or chemical identities [214, 215]. The power of this approach is clear from the experiments of Modungo *et al.* [214] who, after starting with a bicomponent gas of Rb and $^{41}K$ atoms at 300 $\mu$K, were able to produce a 160 nK Bose-Einstein condensate of the $^{41}K$ atoms by forced evaporative cooling of the Rb atoms alone.

Though these techniques may be extended to produce ultracold molecules, their likely effectiveness will depend strongly on the choice of collision partners and the quantum state in which the molecules are trapped. If the molecules are confined in low-field seeking quantum states, as has been the case in most experiments to date, sympathetic cooling will only be possible if elastic collisions (which allow thermalisation) occur much more frequently than inelastic collisions (which eject molecules from the trap). A number of theoretical studies have offered predictions of the relevant cross sections for collisions involving alkali metal atoms, with mostly pessimistic conclusions [216–219].

Inelastic trap loss can be avoided, however, if the molecules are trapped in their ground state, which is possible using AC electric and magnetic fields [78, 179, 220] or an optical dipole trap formed in the focus of an intense off-resonant laser beam [185]. In the first step towards this goal, Schlunk and co-workers have demonstrated the successful transfer of magnetically trapped Rb atoms into an AC electric trap which could be used to confine Stark decelerated ammonia molecules [182, 183]. As the magnetically trapped Rb atoms remain unaffected by the high-frequency electric fields suitable for confining ground state polar molecules, this type of experimental setup should be able to simultaneously trap both species and attempt sympathetic cooling. Barker and co-workers have also suggested sympathetic cooling using ground-state rare gas atoms which are laser-cooled in their metastable states prior to co-trapping with $H_2$ molecules in a deep optical lattice [221].

#### 2. *Trap reloading by irreversible optical pumping*

Higher densities of molecules could conceivably be obtained by repeatedly reloading an electrostatic or magnetic trap. Unfortunately, such a scheme is fundamentally impossible using only conservative forces as changing the trapping potential to admit more molecules necessarily leads to heating or escape of those already trapped. This restriction arises from Liouville's theorem in classical mechanics which only allows the phase-space density to increase through the action of dissipative forces. One possible solution is to use two different trapping fields to simultaneously confine the molecules in different quantum states. If these states can be chosen such that motion in each of the traps is decoupled, the molecules can be transferred from one trapping potential to the other by optical pumping. Reloading is then possible as dissipation is provided by the photons which are emitted during the optical pumping process.

This type of scheme has been proposed for the accumulation of NH radicals using a combination of electrostatic and magnetic trapping fields [62]. The NH molecule is a particularly good candidate: the metastable $a^1\Delta$ state, which can be produced with high efficiency by photolysis of $HN_3$ has a large first-order Stark effect, which permits efficient Stark deceleration and electrostatic trapping [76, 89] After trapping, the molecules can then be optically pumped into the $A^3\Pi$ state, which relaxes efficiently to the $X^3\Sigma^-$ ground state by spontaneous emission [222]. The ground state has only a weak Stark effect, but a strong Zeeman effect, and so the ground-state molecules are not

affected by the switching of the electric trapping fields. The transfer to the ground state occurs in the presence of a magnetic trapping field and this field does not need to be switched off when the next bunch of NH ($a^1\Pi$) molecules is loaded, hence accumulation can occur. Experimental work is currently in progress to demonstrate this final step [76].

Similar ideas have been tested experimentally using laser fields designed to create one-way optical barriers for trapped ultracold atoms [223–225]. Atoms impinging on the barrier from one direction are optically pumped into a quantum state which can be transmitted, whilst those from the other direction remain in a state that is reflected. As such, these experiments provide a physical manifestation of Maxwell's sorting demon [226], allowing spatial compression of the trapped atom cloud or the repeated irreversible transfer of atoms into a different trapping potential.

### 3. *Cavity-assisted laser cooling*

Inside a high-finesse optical cavity, the radiative properties of atoms and molecules are modified relative to those in free-space, allowing rates of spontaneous emission or Raman scattering to be enhanced or suppressed [227]. For example, by tuning a cavity to support a mode with a frequency close to a molecular transition, emission or scattering of photons at the cavity frequency can be promoted. This provides a mechanism for so-called cavity Doppler cooling in which slowly moving molecules are cooled by inelastically scattering photons into one of the cavity modes. The incident photons are provided by a pump laser beam that is red-detuned relative to the mode frequency, whilst cavity-enhancement of the Rayleigh scattering process preferentially causes photons at the frequency of the cavity mode to be produced (see Fig. 11). Cooling occurs through the two-photon Doppler effect: in essence, if the molecules are moving towards the photon source, then backward scattered photons will be blue-shifted with respect to the input light, and the molecules will be slightly slowed. Enhancement of this back-scattering (compared with scattering in the opposite direction which produces red-shifted photons) damps the molecular motion, allowing energy to dissipated by the light leaking stochastically from the cavity.

Unlike conventional laser cooling, where the momentum of the photons is transferred by absorption, cavity-assisted cooling relies on the recoil generated by coherent scattering into the cavity modes. This process is largely independent of the specific energy level structure of the atom or molecule and so the technique may be useful in more complex systems. Moreover, several experiments using ultracold atoms have demonstrated that when large numbers of atoms are introduced into the cavity, unexpectedly large cooling forces have been observed. This has been explained by spontaneous self-organisation in the atom cloud which gives rise to collective Bragg-like scattering behaviour and greatly enhances the cooling rates [228, 229].

For molecules, however, the efficiency of cavity-assisted cooling has yet to be demonstrated. Schemes for cooling OH and CN molecules have been suggested [230–232] but there are a number of inherent practical challenges. The molecules must be confined within the cavity long enough for appreciable cooling to occur, requiring the design of traps compatible with high-finesse optical cavities, which are typically much smaller than the sources currently used to produce cold molecules. Another key factor for cooling molecules will be the control of the molecule-cavity detuning to suppress Raman transitions which populate metastable excited states (which are much less efficiently cooled). In recent work, de Vivie-Riedle and co-workers [230] have proposed manipulating this detuning to drive anti-Stokes Raman transitions to produce ultracold molecules that are cooled in both their translational and internal degrees of freedom. A common feature of a number of cold molecule sources is the production of molecules in rovibrationally excited states; methods capable of quenching this internal exitation may therefore be particularly useful.

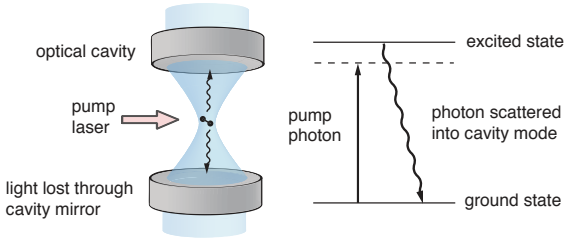


FIG. 11: Cavity-enhanced laser cooling.

## V. EXPERIMENTAL STUDIES OF INELASTIC AND REACTIVE COLLISIONS USING COLD MOLECULE SOURCES

As explained in Section II, the number densities of molecules that can be produced at millikelvin temperatures are typically several orders of magnitude lower than those traditionally employed in crossed molecular beam scattering experiments. Consequently, the experimental observation of very low energy collisions between neutral molecules using molecular beam deceleration or velocity selection techniques is currently a challenging prospect. In particular, the detection of very low numbers of product molecules expected from reactions involving combinations of these types of source provide severe challenges to experimentalists.

Despite these practical difficulties, collisional experiments have begun to be developed. Most notably, van de Meerakker and co-workers were able to perform crossed-beam inelastic scattering experiments using Stark-decelerated OH radicals and a supersonic beam of Xe atoms [82]. The Stark decelerator allowed the contribution of the OH velocity to the collision energy to be continuously varied over the energy range 50 to 400 cm$^{-1}$, whilst the overall kinetic energy resolution was limited to 13 cm$^{-1}$ by the Xe beam. Thresholds for specific energy transfer processes,

$$\mathrm{OH}(X^2\Pi_{3/2}, \nu = 0, J = \tfrac{3}{2}, f) + \mathrm{Xe} \rightarrow \mathrm{OH}(X^2\Pi_{\Omega'}, \nu' = 0, J', e/f) + \mathrm{Xe},$$

were observed, which correspond to changes is the low-lying rotational, spin-orbit, and lambda-doubling levels of the OH molecules. Coupled-channel scattering calculations using *ab initio* diabatic potential surfaces were found to be in excellent agreement with the experimental results, reproducing in particular the relative magnitudes and

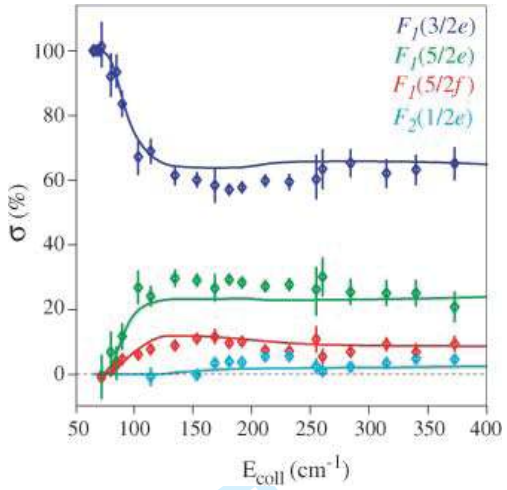


FIG. 12: Collision energy dependence of relative cross sections for inelastic scattering of OH radicals by Xe atoms into various low-lying channels. The solid lines are the results of quantum scattering calculations on two *ab initio* potential surfaces, while the points are from experiments in which the contribution of the OH velocity to the collision energy is varied using a Stark decelerator. From Ref. [82]

near-threshold behaviour of the cross sections, as shown in Fig. 12. Although these experiments involve an energy range that cannot be described as ultracold (or even cold), they demonstrate how Stark-decelerated packets of molecules can be used as highly sensitive probes for long-range intermolecular potential energy surfaces.

A recent similar experiment by Ye and co-workers has investigated the loss of Stark-decelerated OH molecules from a permanent magnet trap by collisions with supersonic beams of He and $D_2$ [195]. The molecules were initially trapped at a temperature of 70 mK and a density of around $10^6$ cm$^{-3}$. By changing the temperature of the pulsed solenoid valve used to produce the supersonic beams, the collision energy could be varied from 60 to 230 cm$^{-1}$ for collisions with He and from 145 to 510 cm$^{-1}$ for collisions involving $D_2$. The deceleration of formaldehyde molecules has also been reported, with the suggestion that reactive collisions of trapped OH and $H_2CO$ could be studied [88]. However prospects for detecting HCO product radicals spectroscopically (*e.g.*, by laser-induced fluorescence) are considered to be "daunting" given the estimated product densities per quantum state.

A possible future approach to collisional studies with Stark decelerated molecules would be to use a version of the molecular synchrotron developed by Heiner *et al.* [83] as a "neutral molecule collider." Pioneering experiments by these authors [70] have shown that it is possible to load two separate bunches of molecules into the split electrostatic hexapole ring which forms the synchrotron. By trapping many more bunches in counterpropagating orbits, the molecules can be made to interact repeatedly on each round trip, potentially giving large increases in the numbers of collisions that can be observed. Additionally, tuning of the synchrotron orbit time can be used to sensitively change the energy of the colliding packets, suggesting that measurements of the energy dependence – and possible resonance-behaviour – of scattering cross sections should be possible.

Inelastic collisions between atoms and molecules have been observed in the ultracold regime using alkali metal systems confined in optical dipole traps [149]. Some of the first detailed measurements of this kind were performed in the groups of Pilet [187] and Weidemüller [233] with $Cs_2$ molecules that were formed by photoassociation and subsequently trapped in the focus of a $CO_2$-laser. Collisions with laser-cooled Cs atoms at characteristic translational temperatures around 50 $\mu$K were seen to cause efficient loss of molecules from the $\sim$2 mK deep trapping potential. The dominant contribution to this loss rate was attributed to vibrational de-excitation of the $Cs_2$ molecules and similar rates were found irrespective of the electronic state used for photoassociation or whether the molecules were initially produced with vibrational quantum numbers in the range $\nu$ = 4 to 6 or $\nu$ = 32 to 47. DeMille and co-workers [188] performed a similar study with heteronuclear RbCs molecules, formed in high vibrational levels of the $a^3\Sigma^+$ state (also by photoassociation). Inelastic collision rates for individual vibrational levels with both Rb and Cs atoms were determined by observing the trap loss over time for different densities of the atomic gases.

The recent demonstration of methods to prepare alkali metal dimers in the lowest rovibrational levels of their electronic ground state is particularly encouraging for these types of experiments and it is likely that new measurements will offer considerable further challenges to theorists studying these systems [234]. But such studies are currently highly restricted in terms of the chemical species that can be used and the potential for reactive studies is perhaps also limited by the difficulty in distinguishing these experimentally from inelastic processes (*e.g.*, the atom exchange reaction between $Cs_2$ and Cs leads to another $Cs_2$ molecule.)

The detection of neutral reaction products generally requires the application of spectroscopic methods, such as laser induced fluorescence, multiphoton ionization or cavity enhanced absorption. In contrast *ionic* products of reactions can generally be detected with very high efficiency using charged particle detectors and mass spectrometric analysis, and in principle single particle sensitivity is achievable. The visibility of individual ions in laser-cooled Coulomb crystals also provides exceptional sensitivity to collisional processes.

In our own work, we have demonstrated these potential benefits in studying the dynamics of ion-neutral reactions at cold or ultracold temperatures. In one of the first experiments to combine two sources of cold atoms/molecules we used a quadrupole velocity selector for neutral dipolar species (see Section IIIB) in conjunction with a laser-cooled radiofrequency ion trap in which $Ca^+$ ions form ordered "Coulomb crystals" (see Section IV.5). As reviewed above (see also [199]), the ions in the crystal are typically spaced by 10–20 $\mu$m and can be stored for hours under UHV conditions. For one dimensional strings of ions localised along the trap axis, the effective temperature is of order of a few millikelvin. The ions are continuously absorbing and emitting photons in the laser cooling process and therefore the fluorescence can be detected and imaged to allow observation of individual ions. In our experiments the trapped calcium ions were exposed to a flux of cold $CH_3F$ from the velocity selector, with translational temperatures in the range 1–4 K, and the reaction $CH_3F + Ca^+ \rightarrow CaF^+ + CH_3$ was monitored through the disappearance of individual $Ca^+$ ions. Absolute rate

constants were measured by calibrating the neutral flux, and the mean collision energy could be varied by changing the voltage applied to the quadrupole velocity selector. The mass-spectrometric detection of $CaF^+$ ions produced from the reaction of $Ca^+$ with $CH_3F$ was also reported; these product ions are trapped and sympathetically cooled into the Coulomb crystal. Although they are dark to the laser induced fluorescence process, the application of an axial radiofrequency field heats up the crystal at specific resonance frequencies which can be related to the masses of the species present.

Such a setup is also extendable to the reactions of molecular ions [129] which can be trapped in the Coulomb crystals by sympathetic cooling [199]. The use of REMPI or pulsed field ionization techniques for production of the ions could potentially enable studies of vibration-rotation selected ions, although the lifetimes of such states are only likely to be compatible with the long trapping times of the ions in selected cases (*e.g.*, non-polar species). The neutral molecules emerging from the quadrupole velocity selector are translationally cold, but are transmitted into the ion trap in a range of vibration-rotation states such that the internal temperature of the neutrals is close to that of the effusive source (*i.e.*, room temperature). If the quadrupole velocity selector was replaced with a Stark decelerator then the measurement of cross sections for *quantum-state selected* neutrals would be possible and a much higher degree of control of the collision energy would also be achieveable. It is likely that reactive collisions could then be studied into the millikelvin range.

The observation of a charge transfer reaction between laser-cooled $Yb^+$ ions in a Paul trap and Yb atoms in a magneto-optical trap has recently been reported [235]. Cross sections were obtained for this process using isotopic substitution at collision energies as low as 400 neV (5 mK); the lower limit of the energy range is determined by the micromotion of the ions in the trap. Good general agreement with the Langevin cross section was obtained over a wide energy range, suggesting that the purely quantum regime had not yet been reached. Indeed at these temperatures around 25 collisional angular momentum states are still active for this reaction.

## VI. THEORY OF CHEMICAL COLLISIONS AT ULTRACOLD TEMPERATURES

In light of the considerable progress that has been made in cold molecule methodology, it is of interest to consider the range of phenomena that might be observed in ultracold chemistry experiments. Figure 13 shows the typical behaviour expected for elastic and reactive (or inelastic) scattering cross sections as a function of collision energy. This particular example shows the results of $s$-wave quantum scattering calculations performed by Hutson and coworkers for the reaction between lithium atoms and their isotopically substituted dimers. At collision energies below 100 $\mu$K, the reactive cross section is seen to increase as the energy is lowered, whilst the elastic cross section becomes constant. This distinctive behaviour is a consequence of the Wigner threshold laws (described in more detail below) which arise from the analytic properties of scattering wavefunctions at low collision energies. Most importantly for ultracold chemistry, these laws predict that the rates of chemical processes do not tend to zero in the limit of vanishingly small collision energies. Above

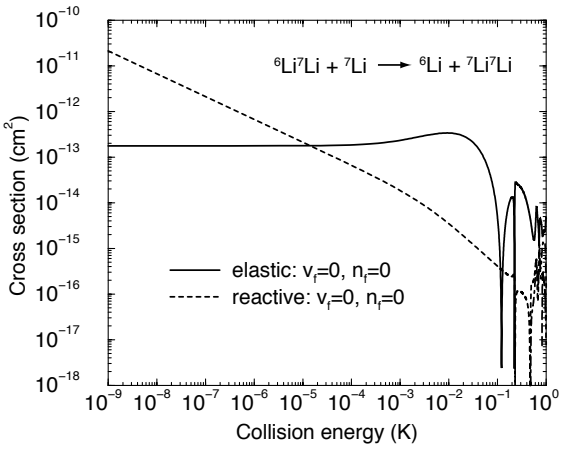


FIG. 13: Elastic and reactive $s$-wave cross sections for $^7$Li + $^6$Li$^7$Li collisions in the cold and ultracold regime. Adapted from Ref [236].

100 mK, both the elastic and reactive cross sections show sharp dependencies on the collision energy. These features are another hallmark trait of cold collisions, which represent the influence of quasibound resonant states whose formation and subsequent decay in the course of the collision produces characteristic signatures in the scattering cross sections.

Before describing some of these effects in more detail, we briefly describe how scattering cross sections for chemical reactions can be calculated quantum mechanically. The fundamental quantity of interest is the so-called $S$-matrix, whose elements are the quantum mechanical probability amplitudes for transitions between a particular quantum state $\alpha$, which specifies the internal rovibronic states of the reactants, into a final product state $\beta$. For collisions occurring in the absence of external fields, the $S$-matrix can be calculated separately for each allowed value of the total angular momentum $J$, which is derived from the vector sum of the orbital angular momentum $l$, and the internal angular momentum of the reactants. State-to-state integral cross sections can be expressed as a sum over the $J$-dependent $S$-matrix elements,

$$\sigma_{\alpha\to\beta}(E_c) = \frac{\pi\hbar^2}{2\mu E_c}\sum_J (2J+1)\left|S^J_{\alpha,\beta}(E_c)\right|^2, \quad (11)$$

where $\mu$ is the reduced mass of the reactants and $E_c$ is the collision energy. For low collision energies, a time-independent approach to solving the Schrödinger equation is the most effective way to calculate the scattering matrices, as the alternative wavepacket approach requires very long propagation times. In general, the scattering wavefunction must be expanded using basis functions which are able to describe simultaneously the collision complex and each of the asymptotic reactant/product channels. This requirement makes reactive scattering calculations very computationally demanding as a large number of coupled-channel equations must be solved to obtain converged cross sections, especially for $J > 0$. For cold collisions in particular, the importance of long-range intermolecular interactions, which require the scattering wavefunction to be propagated to very large distances, together with the need to perform calculations for many partial waves makes the accurate prediction of cross sections a considerable challenge.

In the ultracold limit, the sum in Eq. 11 collapses to include only the $J = 0$ channel as the contributions of higher partial waves are suppressed at long-range by centrifugal barriers in the entrance channel of the reaction. For example, in the lithium atom-dimer reactions considered by Hutson and co-workers, barrier heights of 2.8 and 14.4 mK were found for the $p$-wave and $d$-wave respectively. At temperatures well below these values, the maximum possible size of the ultracold cross section is limited by the incoming flux in the $s$-wave channel, the so-called unitarity limit,

$$\sigma_{\alpha\to\beta}(E_c) \leq \frac{4\pi\hbar^2}{2\mu E_c}. \tag{12}$$

In practice, however, the size of the cross section at low energies depends on the limiting quantum behaviour of the scattering wavefunction, which we describe in the next section.

### 1. *Threshold behaviour, $E_c \to 0$*

The quantum mechanical behaviour of cross sections at low energies was first studied in the context of nuclear reactions caused by neutron scattering. The results of these investigations, which were comprehensively summarised by Wigner [237], can also be applied to atomic and molecular systems in the ultracold regime. For example, in the limit of low collision energies, the cross sections for elastic scattering caused by short-range intermolecular potentials are predicted to vary as,

$$\sigma_l^{\rm el}(k) \sim k^{4l}, \tag{13}$$

where $k$ is the wave-vector associated with the collision energy $E_c = \hbar^2k^2/2\mu$, and $l$ is the orbital angular momentum quantum number of the collision partners. As observed above, elastic cross sections are therefore expected to become constant at low energies.

To provide an illustration of how this particular law arises, we consider the form of the radial wavefunction in the case where there is a single open channel for elastic scattering (see Refs. [238, 239] for more comprehensive treatments). The wavefunction describing the relative motion of the collision partners can be expanded in a basis of eigenfunctions of the orbital angular momentum operator,

$$\Psi(\mathbf{r};k) = \frac{1}{r}\sum_{l=0}^{\infty} A_l\psi_l(r;k)P_l(\cos\theta), \tag{14}$$

where the polynomials, $P_l(\cos\theta)$, are Legendre functions and the radial wavefunctions, $\psi_l(r;k)$, are determined by solving the radial Schrödinger equation,

$$\left[-\frac{\hbar^2}{2\mu}\frac{{\rm d}^2}{{\rm d}r^2} + \frac{l(l+1)\hbar^2}{2\mu r^2} + V(r) - E_c\right]\psi_l(r;k) = 0. \tag{15}$$

Figure 14 shows examples of low collision energy $s$-wave radial wavefunctions calculated for a model potential describing the interaction of two sodium atoms. For very low collision energies, the short-range form of the radial wavefunction is determined almost exclusively by the intermolecular and centrifugal potential. Neglecting the collision energy when solving the radial Schrödinger equation then gives a wavefunction, $\psi_l(r;k=0)$, which in general can only be found by numerical integration. Although at short distances ($r < r_1$) this wavefunction has a complicated oscillatory behaviour caused by the strong intermolecular potential, at larger separations ($r > r_1$) the intermolecular potential vanishes and the wavefunction is then largely determined by the centrifugal potential. In this region the wavefunction can be shown to take the form [240]:

$$\psi_l(r > r_1, k=0) = A\left(r^{l+1} + Br^{-l}\right). \tag{16}$$

where $A$ is a normalisation constant, whilst $B$ is fixed by the short-range solution and remains constant at low energies. At even larger separations, the solutions to the radial Schrödinger equation are homogeneous in $kr$ and are given by a linear combination of the Riccati-Bessel functions. For small values of $kr$ this linear combination can be written as:

$$\psi_l(r;k) = (kr)^{l+1} + \tan\delta_l/(kr)^l, \tag{17}$$

whilst asymptotically the wavefunction resembles a free wave,

$$\psi_l(r\to\infty;k) \sim \sin\left[kr - l\pi/2 + \delta_l(k)\right]. \tag{18}$$

The effect of the interaction potential is therefore conveniently accounted for by the *phase shift*, $\delta_l(k)$. (The phase shift of $l\pi/2$ accounts for the effect of the centrifugal potential alone.) The key part of the argument is that to ensure that the wavefunction of Eq. 17 matches smoothly to that of Eq. 16, the phase-shift is required to behave as,

$$\tan\delta_l \sim k^{2l+1}, \tag{19}$$

which, on substitution into the formula for the elastic cross section,

$$\sigma^{\rm el}(k) = \frac{4\pi}{k^2}\sum_l (2l+1)\sin^2\delta_l(k), \tag{20}$$

gives the low-energy limiting value from the $l = 0$ cross section,

$$\sigma^{\rm el}(k\to 0) = \frac{4\pi a^2}{1+k^2a^2} = 4\pi a^2 + \mathcal{O}(k^2). \tag{21}$$

The constant $a$ is the limiting value of the so-called *scattering length*,

$$a(k) = -\tan\delta_0(k)/k, \tag{22}$$

which can be thought of as the effective "point of origin" [241] of the sinusoidal free wave (see Fig. 14). There are a number of points to be made about this result. Firstly, for collisions between indistinguishable particles the effects of exchange symmetry must be taken into account. In the case of bosons, this symmetry results in the sum of Eq. 20 containing only even values of $l$ and the elastic cross section in Eq. 21 is increased by a factor of 2. For indistinguishable fermions, however, only odd $l$-values are permitted and so elastic scattering becomes forbidden at very low energies. Secondly, the sign and magnitude of the scattering length typically depends very sensitively on the intermolecular potential, in particular on the presence of bound or virtual states near zero energy (although see Ref. [242]). Experience with ultracold atoms has shown that *ab initio* potential curves, in general, cannot be determined with

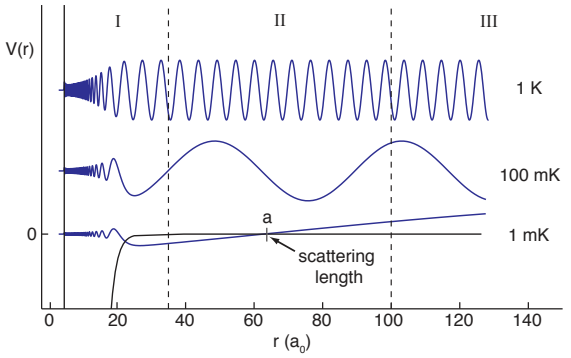


FIG. 14: Radial wavefunctions for $s$-wave scattering at low collision energies. The limiting behaviour of the wavefunction for ultracold collisions in each of the three regions indicated is described in the text.

sufficient accuracy to predict scattering lengths in agreement with those measured experimentally. Thirdly, another consequence of matching Eqs. 16 and 17 is that the amplitude of the short-range wavefunction decreases as the collision energy is lowered, $A \propto k^{l+1}$. This behaviour can be interpreted as a form of quantum reflection [243], which is a uniquely wave-like phenomenon whereby low-energy particles can be reflected even from purely attractive potentials.

Cross sections for inelastic and reactive processes, where the exit channel is energetically lower than the entrance channel, show fundamentally different behaviour from those for elastic scattering. In these channels, the interference between incoming and outgoing waves that is required for quantum reflection does not not occur and the cross sections now behave as,

$$\sigma_l^{\rm in}(k) \sim k^{2l-1}, \qquad (23)$$

and so the low-energy ($s$-wave) dependence is given by,

$$\sigma^{\rm in}(k \to 0) \sim 1/k. \qquad (24)$$

Thus, reactive cross sections at low energies depend inversely on the collision velocity of the reactants. This $1/v$-dependence is well-known in nuclear physics [244] and has the simple interpretation that the probability for reaction is increased by the fact that slowly moving particles spend longer in the interaction potential. Rate constants for exothermic chemical processes, which depend on the product of the cross section with the collision velocity, are therefore constant in the ultracold limit. For many reactions these rate constants will be very small indeed as a result of very low tunnelling rates through reaction barriers. For others, very large rate constants have been predicted, particularly for reactions that are barrierless or where the reaction probabilities can be enhanced by resonance effects and the tunnelling of light atoms. These types of effect are discussed in the next section.

### 2. *Resonance and tunnelling effects in chemical reactions*

A common feature of many scattering processes is the formation of quasi-bound states in which the translational kinetic energy of the collision becomes trapped in the internal modes of a transient collision complex. In reactive systems these types of short-lived resonance states are particularly interesting as they can be localised in regions of the intermolecular potential surface that promote chemical reaction. In such cases, the formation of the quasi-bound wavefunction and subsequent decay into product channels provides a "resonance-mediated" mechanism which can greatly enhance the efficiency of the reaction. For example, following Skodje *et al.* [245], in the absence of direct processes the $J$-dependent state-to-state reaction probability can be described by the Breit-Wigner expression,

$$P^J_{\alpha\to\beta}(E) \propto \frac{\Gamma_\alpha \Gamma_\beta \sqrt{E_\alpha}\sqrt{E_\beta}}{(E - E^J_{\rm res})^2 + \Gamma^2/4}, \qquad (25)$$

where $E_\alpha$ and $E_\beta$ are the translational energies in the reactant and product channels and $\Gamma_\alpha$ and $\Gamma_\beta$ are the widths associated with the formation and decay of the resonance (which has an overall width $\Gamma = \Sigma\Gamma_\gamma$). Thus, for collisions with an energy close to the energy of the resonance, $E \approx E^J_{\rm res}$, large increases in the reaction cross section are expected. Though this behaviour has long been seen in nuclear and particle physics, and also in electron-molecule scattering, unambiguous experimental sightings in chemical systems have been notoriously elusive. (See Ref. [246] for the first theoretically-verified identification of a resonance in the F + HD reaction.)

One reason for the difficulty in detecting resonances in chemical systems is the large number of angular momentum partial waves that typically contribute to collisions at high energies: as resonance states can exist for a broad range of total angular momentum but with slightly different energies ($E^J_{\rm res}$), the experimental signatures of resonant scattering become "washed out." Experiments at very low collision energies are not so severely affected by this kind of impact parameter averaging and competition from non-resonant mechanisms is also expected to be smaller. These two factors suggest that low temperature molecular gases will be a good environment in which to study resonant-scattering processes.

A number of theoretical studies have predicted the occurrence of low-energy resonances in atom-diatom systems such as Cl + HD ($\nu = 1$) [9], Li + HF [247], O($^3$P) + $H_2$ [248] and F + HCl [249]. As Weck and Balakrishnan have emphasised [250], these resonances are typically associated with van der Waals wells on the intermolecular potential surface. Although these regions lie far from the reaction transition state, the long duration of the low energy collision allows formation of "pre-reactive" states which preferentially decay by tunnelling through the reaction barrier. Similarly, calculations by Bowman and co-workers have shown that tunnelling can also be promoted by van der Waals minima in the exit channels of reactions [251, 252]. It should be noted that the energy-scale of van der Waals resonances places them in the cold regime (and above), where a reasonably large number of partial waves still contribute to reaction cross sections. Most calculations performed to date have consider only the lowest values of the total angular momentum and so it remains to be seen whether these types of resonance can be be resolved experimentally.

A different indication of near-resonance scattering has been predicted by Bodo and co-workers [253] who calculated a very large zero-energy rate constant for the F + $H_2$ reaction, which was attributed to the presence of a virtual state near threshold. By artificially tuning the mass of the H-atoms, a marked change in the value of the rate constant

could be observed as the virtual state was brought closer to zero-energy. These calculations also revealed a pronounced Ramsauer-Townsend minimum in the elastic scattering cross section, caused by the sinusoidal dependence on the phase shift at low energies (see Eq. 20). This result is particularly interesting as the observation of this quantum mechanical phenomenon in molecular systems has so far been limited to electron-molecule scattering.

In the ultracold regime, numerous Feshbach resonances associated with the hyperfine structure of molecules are also expected to occur. Although these types of resonance are difficult to include in quantum scattering calculations as many sources of angular momentum must be coupled, indications of their existence have already been seen in the experiments of Grimm and co-workers [149]. Optically trapped $Cs_2$ molecules levitated against gravity by an external magnetic field were observed to undergo large inelastic loss rates as the magnetic field was tuned. In direct analogy with the Feshbach resonances seen for ultracold atomic dimers, these losses were attributed to coupling of the continuum scattering state of the two molecules with the highest-lying bound states of the $Cs_4$ tetramer.

### 3. *External field control*

As the energy scale of long-range intermolecular interactions can be of the same order of magnitude as the Stark or Zeeman shifts experienced by molecules in laboratory-strength fields, it has been suggested that external electric or magnetic fields might be used to control chemical collisions in low temperature gases [11]. A number of effects have been predicted. Krems and co-workers calculated that weakly-bound van der Waals molecules could be dissociated using a magnetic field [254], while Bohn and co-workers have predicted the existence of scattering resonances in collisions of polar molecules in an external electric field [255]. These resonances are caused by long-range "field-linked" states occurring near threshold in the field-dressed dipole-dipole potential and it has been suggested that these states can be used to suppress the occurrence of short-range collisions that are needed for chemical reaction [88]. Experimental and theoretical progress in the area of "Cold controlled chemistry" has been recently reviewed by Krems [12].

## VII. CONCLUSION AND FUTURE PROSPECTS

Despite the very considerable progress that has been made in the development of experimental techniques for producing cold and ultracold molecular species, the field of ultralow energy collisions using such species remains very much in its infancy at the time of writing. Theoretical work to date has highlighted the range of potentially interesting effects that could be observed in these temperature ranges, but such predictions await experimental verification. The comparison between experiment and theory is one of the key aspects of interest in this field, and there is a need for experimentalists and theoreticians to find chemical systems that are both theoretically and experimentally tractable. Thus for example, the interesting calculations of cross sections for the $F + H_2$ reaction may remain untested for a considerable time, as neither of these reactants have been cooled or decelerated in their ground states. On the theoretical side, one of the major challenges is the sensitivity of predicted collision cross section to the accuracy of the intermolecular potential, and the non-adiabatic long-range behaviour of the system for open-shell species where multiple surfaces converge at long range. In addition the calculation of cross sections at 1 K needs to take into account the multiple partial waves contributing to the scattering. Such considerations currently limit the number of systems for which accurate calculations can be performed.

The key experimental challenges for the future include: the optimisation of decelerators to produce higher fluxes of cold molecules; the implementation of sympathetic cooling schemes for neutral species; the development of traps (electric/magnetic, optical, microwave) for ground state molecules that can be loaded with sufficient number densities for evaporative cooling; the implementation of cavity cooling schemes for molecules; the optimisation of coherent control schemes for producing molecules in their rovibrational ground states that were initially formed in highly excited states by association of cold atoms; the development of ultrahigh sensitivity detection schemes for neutral molecules; the refinement of methods for studying collisions of single trapped ions, and the use of sideband cooling to reduce the temperature.

There are exciting technological developments taking place in this area of research, many of which are likely to have spin-offs into other areas. For example, the use of a Stark or Zeeman decelerator as a high-energy-resolution, quantum-state-selected source of molecules for collisional studies is potentially valuable in reaction dynamics and beam-surface scattering studies over a very wide range of temperatures, not just limited to the cold and ultracold regimes.

Finally, although this article has focused on potential applications of ultracold molecules in the study of chemical collisions, there are many other potential applications in chemistry and physics which will drive progress in this area. These applications include: the use of cold molecule sources in high resolution spectroscopy, where the reduced Doppler width and reduced transit time broadening is advantageous; the application of high resolution spectroscopy to tests of fundamental physics (*e.g.*, time variation of fundamental constants); the direct measurement of long radiative lifetimes and other decay processes; the study of Bose-Einstein condensation using molecular and dipolar species, and the link to condensed matter physics; the application of optically trapped arrays of molecules to quantum computation devices; the use of electromagnetic and optical fields for control of molecular properties, including the development of miniaturized devices.

### Acknowledgments

We are grateful to the EPSRC for supporting our work in the field of cold molecules, and for a studentship for MB. We also acknowledge the contributions of Dr. David Carty and Dr. Simon Procter to the Stark deceleration work in Section IIIA.

[1] K. Southwell, Nature **416**, 205 (2002).
[2] I. Bloch, J. Dalibard, and W. Zwerger, Rev. Mod. Phys. **80**, 885 (2008).
[3] C. Monroe, Nature **416**, 238 (2002).
[4] O. Dulieu, M. Raoult, and E. Tiemann, J Phys B-At Mol Opt **39**, (19) Introductory Review (2006).
[5] J. Doyle, B. Friedrich, R. V. Krems, and F. Masnou-Seeuws, Eur Phys J D **31**, 149 (2004).
[6] C. Pethick and H. Smith, *Bose-Einstein Condensation in Dilute Gases* (Cambridge University Press, Cambridge, 2008).
[7] E. Herbst, Chem Soc Rev **30**, 168 (2001).
[8] R. Sahai and L. A. Nyman, Astrophys J Lett **487**, L155 (1997).
[9] N. Balakrishnan, J. Chem. Phys. **121**, 5563 (2004).
[10] D. Skouteris, D. E. Manolopoulos, W. S. Bian, H. J. Werner, L. H. Lai, and K. P. Liu, Science **286**, 1713 (1999).
[11] R. V. Krems, Int. Rev. Phys. Chem. **24**, 99 (2005).
[12] R. V. Krems, Phys. Chem. Chem. Phys. **10**, 4079 (2008).
[13] S. C. Althorpe and D. C. Clary, Annu. Rev. Phys. Chem. **54**, 493 (2003).
[14] J. van Veldhoven, J. Küpper, H. L. Bethlem, B. Sartakov, A. J. A. van Roij, and G. Meijer, Eur Phys J D **31**, 337 (2004).
[15] J. C. J. Koelemeij, B. Roth, A. Wicht, I. Ernsting, and S. Schiller, Phys. Rev. Lett. **98**, 173002 (2007).
[16] J. J. Hudson, B. E. Sauer, M. R. Tarbutt, and E. A. Hinds, Phys. Rev. Lett. **89**, 023003 (2002).
[17] M. Quack, J. Stohner, and M. Willeke, Annu. Rev. Phys. Chem. **59**, 741 (2008).
[18] E. R. Hudson, H. J. Lewandowski, B. C. Sawyer, and J. Ye, Phys. Rev. Lett. **96**, 143004 (2006).
[19] M. T. Murphy, V. V. Flambaum, S. Muller, and C. Henkel, Science **320**, 1611 (2008).
[20] L. Santos, G. V. Shlyapnikov, P. Zoller, and M. Lewenstein, Phys. Rev. Lett. **85**, 1791 (2000).
[21] T. Lahaye, T. Koch, B. Froehlich, M. Fattori, J. Metz, A. Griesmaier, S. Giovanazzi, and T. Pfau, Nature **448**, 672 (2007).
[22] D. J. Heinzen, R. Wynar, P. D. Drummond, and K. V. Kheruntsyan, Phys. Rev. Lett. **84**, 5029 (2000).
[23] M. G. Moore and A. Vardi, Phys. Rev. Lett. **88**, 160402 (2002).
[24] V. V. Flambaum and J. S. M. Ginges, Phys. Rev. A **74**, 025601 (2006).
[25] D. DeMille, Phys. Rev. Lett. **88**, 067901 (2002).
[26] A. Micheli, G. K. Brennen, and P. Zoller, Nat. Phys. **2**, 341 (2006).
[27] D. G. Truhlar, B. C. Garrett, and S. J. Klippenstein, J Phys Chem **100**, 12771 (1996).
[28] I. W. M. Smith, Chem Soc Rev **37**, 812 (2008).
[29] D. C. Clary, Annu. Rev. Phys. Chem. **41**, 61 (1990).
[30] D. Carty, A. Goddard, S. P. K. Kohler, I. R. Sims, and I. W. M. Smith, J Phys Chem A **110**, 3101 (2006).
[31] J. A. Kłos, F. Lique, M. H. Alexander, and P. J. Dagdigian, J. Chem. Phys. **129**, 064306 (2008).
[32] E. Buonomo and D. C. Clary, J Phys Chem A **105**, 2694 (2001).
[33] R. I. Kaiser, D. Stranges, Y. T. Lee, and A. G. Suits, Astrophys J **477**, 982 (1997).
[34] S. R. Mackenzie and T. P. Softley, J. Chem. Phys. **101**, 10609 (1994).
[35] S. Willitsch, M. T. Bell, A. D. Gingell, S. R. Procter, and T. P. Softley, Phys. Rev. Lett. **100**, 043203 (2008).
[36] R. D. Guettler, G. C. Jones, L. A. Posey, and R. N. Zare, Science **266**, 259 (1994).
[37] R. Macdonald and K. Liu, J. Chem. Phys. **93**, 2443 (1990).
[38] I. R. Sims, J. L. Queffelec, A. Defrance, C. RebrionRowe, D. Travers, B. R. Rowe, and I. W. M. Smith, J. Chem. Phys. **97**, 8798 (1992).
[39] R. W. Fair and B. A. Thrush, Trans. Faraday Soc. **65**, 1557 (1969).
[40] M. Y. Ballester and A. J. C. Varandas, Chem. Phys. Lett. **433**, 279 (2007).
[41] I. R. Sims, I. W. M. Smith, D. C. Clary, P. Bocherel, and B. R. Rowe, J. Chem. Phys. **101**, 1748 (1994).
[42] M. B. Arfa, B. Lescop, M. Cherid, B. Brunetti, P. Candori, D. Malfatti, S. Falcinelli, and F. Vecchiocattivi, Chem. Phys. Lett. **308**, 71 (1999).
[43] P. E. Siska, Rev. Mod. Phys. **65**, 337 (1993).
[44] S. T. Pratt, J. L. Dehmer, P. M. Dehmer, and W. A. Chupka, J. Chem. Phys. **101**, 882 (1994).
[45] T. P. Softley, Int. Rev. Phys. Chem. **23**, 1 (2004).
[46] T. V. Tscherbul, Ğ. Barinovs, J. Kłos, and R. V. Krems, Phys. Rev. A **78**, 7 (2008).
[47] S. Jung, E. Tiemann, and C. Lisdat, Phys. Rev. A **74**, 040701 (2006).
[48] O. Bucicov, M. Nowak, S. Jung, G. Meijer, E. Tiemann, and C. Lisdat, Eur Phys J D **46**, 463 (2008).
[49] A. C. Terentis, S. E. Waugh, G. F. Metha, and S. H. Kable, J. Chem. Phys. **108**, 3187 (1998).
[50] E. E. Ferguson, Annu. Rev. Phys. Chem. **26**, 17 (1975).
[51] D. C. Clary and J. P. Henshaw, Faraday Discuss **84**, 333 (1987).
[52] J. Troe, J. Chem. Phys. **87**, 2773 (1987).
[53] I. W. M. Smith, Angew. Chem. Int. Ed. **45**, 2842 (2006).
[54] A. W. Jasper, C. Y. Zhu, S. Nangia, and D. G. Truhlar, Faraday Discuss **127**, 1 (2004).
[55] P. Soldan, M. T. Cvitas, J. M. Hutson, P. Honvault, and J. M. Launay, Phys. Rev. Lett. **89**, 153201 (2002).
[56] G. Scoles, *Atomic and molecular beam methods. Vol. 1* (Oxford University Press, Oxford, 1988).
[57] L. K. Randeniya, X. K. Zeng, and M. A. Smith, Chem. Phys. Lett. **147**, 346 (1988).
[58] I. R. Sims and I. W. M. Smith, Annu. Rev. Phys. Chem. **46**, 109 (1995).
[59] D. Carty, V. L. Page, I. R. Sims, and I. W. M. Smith, Chem. Phys. Lett. **344**, 310 (2001).
[60] H. J. Metcalf and P. van der Straten, *Laser Cooling and Trapping* (Springer-Verlag, New York, 1999).
[61] B. K. Stuhl, B. C. Sawyer, and D. Wang, arXiv **physics.atom-ph** (2008).
[62] S. Y. T. van de Meerakker, R. T. Jongma, H. L. Bethlem, and G. Meijer, Phys. Rev. A **64**, 041401 (2001).
[63] M. D. D. Rosa, Eur Phys J D **31**, 395 (2004).
[64] D. J. Tannor, R. Kosloff, and A. Bartana, Faraday Discuss **113**, 365 (1999).
[65] H. L. Bethlem, G. Berden, and G. Meijer, Phys. Rev. Lett. **83**, 1558 (1999).
[66] H. L. Bethlem and G. Meijer, Int. Rev. Phys. Chem. **22**, 73 (2003).
[67] S. Y. T. van de Meerakker, N. Vanhaecke, H. L. Bethlem, and G. Meijer, Phys. Rev. A **71**, 053409 (2005).
[68] K. Gubbels, G. Meijer, and B. Friedrich, Phys. Rev. A **73**, 063406 (2006).
[69] B. C. Sawyer, B. K. Stuhl, B. L. Lev, J. Ye, and E. R. Hudson, Eur Phys J D **48**, 197 (2008).
[70] C. E. Heiner, H. L. Bethlem, and G. Meijer, Phys. Chem. Chem. Phys. **8**, 2666 (2006).
[71] F. M. H. Crompvoets, R. T. Jongma, H. L. Bethlem, A. J. A. van Roij, and G. Meijer, Phys. Rev. Lett. **89**, 093004 (2002).
[72] S. Y. T. van de Meerakker, N. Vanhaecke, M. P. J. van der Loo, G. C. Groenenboom, and G. Meijer, Phys. Rev. Lett. **95**, 013003 (2005).
[73] J. J. Gilijamse, S. Hoekstra, S. A. Meek, M. Metsälä, S. Y. T. van de Meerakker, G. Meijer, and G. C. Groenenboom, J. Chem. Phys. **127**, 221102 (2007).

[74] H. L. Bethlem, G. Berden, F. M. H. Crompvoets, R. T. Jongma, A. J. A. van Roij, and G. Meijer, Nature **406**, 491 (2000).
[75] S. Y. T. van de Meerakker, P. H. M. Smeets, N. Vanhaecke, R. T. Jongma, and G. Meijer, Phys. Rev. Lett. **94**, 023004 (2005).
[76] S. Hoekstra, M. Metsälä, P. C. Zieger, L. Scharfenberg, J. J. Gilijamse, G. Meijer, and S. Y. T. van de Meerakker, Phys. Rev. A **76**, 063408 (2007).
[77] H. L. Bethlem, J. van Veldhoven, M. Schnell, and G. Meijer, Phys. Rev. A **74**, 063403 (2006).
[78] M. Schnell, P. Lutzow, J. van Veldhoven, H. L. Bethlem, J. Küpper, B. Friedrich, M. Schleier-Smith, H. Haak, and G. Meijer, J Phys Chem A **111**, 7411 (2007).
[79] B. C. Sawyer, B. L. Lev, E. R. Hudson, B. K. Stuhl, M. Lara, J. L. Bohn, and J. Ye, Phys. Rev. Lett. **98**, 253002 (2007).
[80] S. A. Schulz, H. L. Bethlem, J. van Veldhoven, J. Küpper, H. Conrad, and G. Meijer, Phys. Rev. Lett. **93**, 020406 (2004).
[81] M. Metsälä, J. J. Gilijamse, S. Hoekstra, S. van de Meerakker, and G. Meijer, New J. Phys. **10**, 053018 (2008).
[82] J. J. Gilijamse, S. Hoekstra, S. Y. T. van de Meerakker, G. C. Groenenboom, and G. Meijer, Science **313**, 1617 (2006).
[83] C. E. Heiner, D. Carty, G. Meijer, and H. L. Bethlem, Nat. Phys. **3**, 115 (2007).
[84] H. L. Bethlem, F. M. H. Crompvoets, R. T. Jongma, S. Y. T. van de Meerakker, and G. Meijer, Phys. Rev. A **65**, 053416 (2002).
[85] J. R. Bochinski, E. R. Hudson, H. J. Lewandowski, G. Meijer, and J. Ye, Phys. Rev. Lett. **91**, 243001 (2003).
[86] S. Y. T. van de Meerakker, N. Vanhaecke, and G. Meijer, Annu. Rev. Phys. Chem. **57**, 159 (2006).
[87] S. Hoekstra, J. J. Gilijamse, B. Sartakov, N. Vanhaecke, L. Scharfenberg, S. Y. T. van de Meerakker, and G. Meijer, Phys. Rev. Lett. **98**, 133001 (2007).
[88] E. R. Hudson, C. Ticknor, B. C. Sawyer, C. A. Taatjes, H. J. Lewandowski, J. R. Bochinski, J. L. Bohn, and J. Ye, Phys. Rev. A **73**, 063404 (2006).
[89] S. Y. T. van de Meerakker, I. Labazan, S. Hoekstra, J. Küpper, and G. Meijer, J Phys B-At Mol Opt **39**, S1077 (2006).
[90] S. Y. T. van de Meerakker, H. L. Bethlem, and G. Meijer, Nat. Phys. **4**, 595 (2008).
[91] D. Auerbach, E. E. Bromberg, and L. Wharton, J. Chem. Phys. **45**, 2160 (1966).
[92] H. L. Bethlem, A. J. A. van Roij, R. T. Jongma, and G. Meijer, Phys. Rev. Lett. **88**, 133003 (2002).
[93] K. Wohlfart, F. Grätz, F. Filsinger, H. Haak, G. Meijer, and J. Küpper, Phys. Rev. A **77**, 031404 (2008).
[94] K. Wohlfart, F. Filsinger, F. Graetz, J. Küpper, and G. Meijer, Phys. Rev. A **78**, 033421 (2008).
[95] M. R. Tarbutt, H. L. Bethlem, J. J. Hudson, V. L. Ryabov, V. A. Ryzhov, B. E. Sauer, G. Meijer, and E. A. Hinds, Phys. Rev. Lett. **92**, 173002 (2004).
[96] H. L. Bethlem, M. R. Tarbutt, J. Küpper, D. Carty, K. Wohlfart, E. A. Hinds, and G. Meijer, J Phys B-At Mol Opt **39**, R263 (2006).
[97] M. R. Tarbutt and E. A. Hinds, New J. Phys. **10**, 073011 (2008).
[98] N. Vanhaecke, U. Meier, M. Andrist, B. H. Meier, and F. Merkt, Phys. Rev. A **75**, 031402 (2007).
[99] E. Narevicius, C. G. Parthey, A. Libson, J. Narevicius, I. Chavez, U. Even, and M. G. Raizen, New J. Phys. **9**, 358 (2007).
[100] S. D. Hogan, D. Sprecher, M. Andrist, and N. Vanhaecke, Phys. Rev. A **76**, 023412 (2007).
[101] E. Narevicius, A. Libson, C. G. Parthey, I. Chavez, J. Narevicius, U. Even, and M. G. Raizen, Phys. Rev. Lett. **100**, 093003 (2008).
[102] E. Narevicius, A. Libson, C. G. Parthey, I. Chavez, J. Narevicius, U. Even, and M. G. Raizen, Phys. Rev. A **77**, 051401 (2008).
[103] S. D. Hogan, A. W. Wiederkehr, H. Schmutz, and F. Merkt, Phys. Rev. Lett. **101**, 143001 (2008).
[104] S. R. Procter, Y. Yamakita, F. Merkt, and T. P. Softley, Chem. Phys. Lett. **374**, 667 (2003).
[105] Y. Yamakita, S. R. Procter, A. L. Goodgame, T. P. Softley, and F. Merkt, J. Chem. Phys. **121**, 1419 (2004).
[106] E. Vliegen and F. Merkt, Phys. Rev. Lett. **97**, 033002 (2006).
[107] E. Vliegen, S. D. Hogan, H. Schmutz, and F. Merkt, Phys. Rev. A **76**, 023405 (2007).
[108] S. D. Hogan and F. Merkt, Phys. Rev. Lett. **100**, 043001 (2008).
[109] E. Vliegen, H. J. Wörner, T. P. Softley, and F. Merkt, Phys. Rev. Lett. **92**, 033005 (2004).
[110] D. Jaksch, J. I. Cirac, P. Zoller, S. L. Rolston, R. Cote, and M. D. Lukin, Phys. Rev. Lett. **85**, 2208 (2000).
[111] M. Saffman and K. Molmer, Phys. Rev. A **78**, 012336 (2008).
[112] C. H. Greene, A. S. Dickinson, and H. R. Sadeghpour, Phys. Rev. Lett. **85**, 2458 (2000).
[113] H. Stapelfeldt, H. Sakai, E. Constant, and P. Corkum, Phys. Rev. Lett. **79**, 2787 (1997).
[114] P. F. Barker, S. M. Purcell, and M. N. Shneider, Phys. Rev. A **77**, 063409 (2008).
[115] R. Fulton, A. I. Bishop, and P. F. Barker, Phys. Rev. A **71**, 4 (2005).
[116] R. Fulton, A. I. Bishop, and P. F. Barker, Phys. Rev. Lett. **93**, 243004 (2004).
[117] G. Dong, S. Edvadsson, W. Lu, and P. F. Barker, Phys. Rev. A **72**, 4 (2005).
[118] B. S. Zhao, S. H. Lee, H. S. Chung, S. Hwang, W. K. Kang, B. Friedrich, and D. S. Chung, J. Chem. Phys. **119**, 8905 (2003).
[119] P. B. Corkum, C. Ellert, M. Mehendale, P. Dietrich, S. Hankin, S. Aseyev, D. Rayner, and D. Villeneuve, Faraday Discuss **113**, 47 (1999).
[120] R. Fulton, A. I. Bishop, M. N. Shneider, and P. F. Barker, Nat Phys **2**, 465 (2006).
[121] R. Fulton, A. I. Bishop, M. N. Shneider, and P. F. Barker, J Phys B-At Mol Opt **39**, S1097 (2006).
[122] J. Ramirez-Serrano, K. E. Strecker, and D. W. Chandler, Phys. Chem. Chem. Phys. **8**, 2985 (2006).
[123] P. B. Moon, C. T. Rettner, and J. P. Simons, J Chem Soc Faraday Trans **74**, 630 (1978).
[124] M. Gupta and D. Herschbach, J Phys Chem A **103**, 10670 (1999).
[125] M. Gupta and D. Herschbach, J. Phys. Chem. A **105**, 1626 (2001).
[126] E. Narevicius, A. Libson, M. F. Riedel, C. G. Parthey, I. Chavez, U. Even, and M. G. Raizen, Phys. Rev. Lett. **98**, 103201 (2007).
[127] S. A. Rangwala, T. Junglen, T. Rieger, P. W. H. Pinkse, and G. Rempe, Phys. Rev. A **67**, 043406 (2003).
[128] T. Junglen, T. Rieger, S. A. Rangwala, P. W. H. Pinkse, and G. Rempe, Eur Phys J D **31**, 365 (2004).
[129] M. T. Bell, A. D. Gingell, J. Oldham, T. P. Softley, and S. Willitsch, Faraday Discuss **142** (2008) (accepted).
[130] M. Motsch, M. Schenk, L. D. van Buuren, M. Zeppenfeld, P. W. H. Pinkse, and G. Rempe, Phys. Rev. A **76**, 061402 (2007).
[131] T. Rieger, T. Junglen, S. A. Rangwala, P. W. H. Pinkse, and G. Rempe, Phys. Rev. Lett. **95**, 173002 (2005).
[132] F. Filsinger, U. Erlekam, G. von Helden, J. Küpper, and G. Meijer, Phys. Rev. Lett. **100**, 133003 (2008).
[133] D. Patterson and J. M. Doyle, J. Chem. Phys. **126**, 154307 (2007).
[134] S. E. Maxwell, N. Brahms, R. deCarvalho, D. R. Glenn, J. S. Helton, S. V. Nguyen, D. Patterson, J. Petricka, D. DeMille, and J. M. Doyle, Phys. Rev. Lett. **95**, 173201 (2005).

[135] L. D. van Buuren, C. Sommer, M. Motsch, S. Pohle, M. Schenk, J. Bayerl, P. W. H. Pinkse, and G. Rempe, arXiv **physics.chem-ph** (2008).
[136] S. Deachapunya, P. J. Fagan, A. G. Major, E. Reiger, H. Ritsch, A. Stefanov, H. Ulbricht, and M. Arndt, Eur Phys J D **46**, 307 (2008).
[137] J. M. Hutson and P. Soldan, Int. Rev. Phys. Chem. **25**, 497 (2006).
[138] T. Bourdel, L. Khaykovich, J. Cubizolles, J. Zhang, F. Chevy, M. Teichmann, L. Tarruell, S. J. J. M. F. Kokkelmans, and C. Salomon, Phys. Rev. Lett. **93**, 050401 (2004).
[139] M. Greiner, C. A. Regal, and D. S. Jin, Nature **426**, 537 (2003).
[140] K. M. Jones, Rev. Mod. Phys. **78**, 483 (2006).
[141] J. M. Sage, S. Sainis, T. Bergeman, and D. DeMille, Phys. Rev. Lett. **94**, 203001 (2005).
[142] C. P. Koch, J. P. Palao, R. Kosloff, and F. Masnou-Seeuws, Phys. Rev. A **70**, 013402 (2004).
[143] S. Durr, T. Volz, A. Marte, and G. Rempe, Phys. Rev. Lett. **92**, 020406 (2004).
[144] T. Koehler, K. Goral, and P. S. Julienne, Rev. Mod. Phys. **78**, 1311 (2006).
[145] F. Lang, P. V. D. Straten, B. Brandstaetter, G. Thalhammer, K. Winkler, P. S. Julienne, R. Grimm, and J. H. Denschlag, Nat. Phys. **4**, 223 (2008).
[146] F. Ferlaino, S. Knoop, M. Mark, M. Berninger, H. Schoebel, H.-C. Nägerl, and R. Grimm, Phys. Rev. Lett. **101**, 023201 (2008).
[147] T. Kraemer, M. Mark, P. Waldburger, J. Danzl, C. Chin, B. Engeser, A. D. Lange, K. Pilch, A. Jaakkola, H.-C. Nägerl, et al., Nature **440**, 315 (2006).
[148] K. Xu, T. Mukaiyama, J. Abo-Shaeer, J. Chin, D. Miller, and W. Ketterle, Phys. Rev. Lett. **91**, 210402 (2003).
[149] C. Chin, T. Kraemer, M. Mark, J. Herbig, P. Waldburger, H.-C. Nägerl, and R. Grimm, Phys. Rev. Lett. **94**, 123201 (2005).
[150] J. Deiglmayr, A. Grochola, M. Repp, K. Mörtlbauer, C. Glück, J. Lange, O. Dulieu, R. Wester, and M. Weidemüller, Phys. Rev. Lett. **101**, 4 (2008).
[151] M. Viteau, A. Chotia, M. Allegrini, N. Bouloufa, O. Dulieu, D. Comparat, and P. Pillet, Science **321**, 232 (2008).
[152] F. Lang, K. Winkler, C. Strauss, R. Grimm, and J. H. Denschlag, Phys. Rev. Lett. **101**, 4 (2008).
[153] K. K. Ni, S. Ospelkaus, M. H. G. de Miranda, A. Pe'er, B. Neyenhuis, J. J. Zirbel, S. Kotochigova, P. S. Julienne, D. S. Jin, and J. Ye, Science **322**, 231 (2008).
[154] J. D. Weinstein, R. deCarvalho, T. Guillet, B. Friedrich, and J. M. Doyle, Nature **395**, 148 (1998).
[155] J. M. Bakker, M. Stoll, D. R. Weise, O. Vogelsang, G. Meijer, and A. Peters, J Phys B-At Mol Opt **39**, S1111 (2006).
[156] R. deCarvalho, J. M. Doyle, B. Friedrich, T. Guillet, J. Kim, D. Patterson, and J. D. Weinstein, Eur Phys J D **7**, 289 (1999).
[157] J. G. E. Harris, R. A. Michniak, S. V. Nguyen, W. C. Campbell, D. Egorov, S. E. Maxwell, L. D. van Buuren, and J. M. Doyle, Rev Sci Instrum **75**, 17 (2004).
[158] J. D. Weinstein, R. deCarvalho, K. Amar, A. Boca, B. C. Odom, B. Friedrich, and J. M. Doyle, J. Chem. Phys. **109**, 2656 (1998).
[159] W. C. Campbell, E. Tsikata, H.-I. Lu, L. D. van Buuren, and J. M. Doyle, Phys. Rev. Lett. **98**, 213001 (2007).
[160] M. Stoll, J. M. Bakker, T. C. Steimle, G. Meijer, and A. Peters, Phys. Rev. A **78**, 032707 (2008).
[161] J. G. E. Harris, R. A. Michniak, S. V. Nguyen, N. Brahms, W. Ketterle, and J. M. Doyle, Europhys Lett **67**, 198 (2004).
[162] C. I. Hancox, S. C. Doret, M. T. Hummon, L. J. Luo, and J. M. Doyle, Nature **431**, 281 (2004).
[163] S. V. Nguyen, J. S. Helton, K. Maussang, W. Ketterle, and J. M. Doyle, Phys. Rev. A **71**, 025602 (2005).
[164] S. V. Nguyen, S. C. Doret, C. B. Connolly, R. A. Michniak, W. Ketterle, and J. M. Doyle, Phys. Rev. A **72**, 060703 (2005).
[165] C. I. Hancox, M. T. Hummon, S. V. Nguyen, and J. M. Doyle, Phys. Rev. A **71**, 031402 (2005).
[166] J. G. E. Harris, S. V. Nguyen, S. C. Doret, W. Ketterle, and J. M. Doyle, Phys. Rev. Lett. **99**, 223201 (2007).
[167] S. V. Nguyen, R. deCarvalho, and J. M. Doyle, Phys. Rev. A **75**, 062706 (2007).
[168] J. P. Toennies and A. F. Vilesov, Angew Chem Int Edit **43**, 2622 (2004).
[169] A. Scheidemann, J. P. Toennies, and J. A. Northby, Phys. Rev. Lett. **64**, 1899 (1990).
[170] M. Hartmann, R. E. Miller, J. P. Toennies, and A. F. Vilesov, Science **272**, 1631 (1996).
[171] D. S. Peterka, J. H. Kim, C. C. Wang, and D. M. Neumark, J Phys Chem B **110**, 19945 (2006).
[172] M. Farnik and J. P. Toennies, J. Chem. Phys. **122**, 014307 (2005).
[173] E. Lugovoj, J. Toennies, and A. Vilesov, J. Chem. Phys. **112**, 8217 (2000).
[174] M. Elioff, J. Valentini, and D. Chandler, The European Physical Journal D-Atomic **31**, 385 (2004).
[175] M. S. Elioff, J. J. Valentini, and D. W. Chandler, Science **302**, 1940 (2003).
[176] N. Liu and H. Loesch, Phys. Rev. Lett. **98**, 103002 (2007).
[177] S. J. Matthews, S. Willitsch, and T. P. Softley, Phys. Chem. Chem. Phys. **9**, 5656 (2007).
[178] J. J. Gilijamse, J. Küpper, S. Hoekstra, N. Vanhaecke, S. Y. T. van de Meerakker, and G. Meijer, Phys. Rev. A **73**, 063410 (2006).
[179] J. van Veldhoven, H. L. Bethlem, M. Schnell, and G. Meijer, Phys. Rev. A **73**, 063408 (2006).
[180] J. Kleinert, C. Haimberger, P. J. Zabawa, and N. P. Bigelow, Phys. Rev. Lett. **99**, 143002 (2007).
[181] R. T. Jongma, G. vonHelden, G. Berden, and G. Meijer, Chem. Phys. Lett. **270**, 304 (1997).
[182] S. Schlunk, A. Marian, P. Geng, A. P. Mosk, G. Meijer, and W. Schöllkopf, Phys. Rev. Lett. **98**, 223002 (2007).
[183] S. Schlunk, A. Marian, W. Schöllkopf, and G. Meijer, Phys. Rev. A **77**, 043408 (2008).
[184] T. Rieger, P. Windpassinger, S. A. Rangwala, G. Rempe, and P. W. H. Pinkse, Phys. Rev. Lett. **99**, 063001 (2007).
[185] T. Takekoshi, B. M. Patterson, and R. J. Knize, Phys. Rev. Lett. **81**, 5105 (1998).
[186] R. Grimm, M. Weidemüller, and Y. B. Ovchinnikov, Adv Atom Mol Opt Phy **42**, 95 (2000).
[187] N. Zahzam, T. Vogt, M. Mudrich, D. Comparat, and P. Pillet, Phys. Rev. Lett. **96**, 023202 (2006).
[188] E. R. Hudson, N. B. Gilfoy, S. Kotochigova, J. M. Sage, and D. DeMille, Phys. Rev. Lett. **100**, 203201 (2008).
[189] G. Thalhammer, K. Winkler, F. Lang, S. Schmid, R. Grimm, and J. H. Denschlag, Phys. Rev. Lett. **96**, 050402 (2006).
[190] T. Rom, T. Best, O. Mandel, A. Widera, M. Greiner, T. W. Hansch, and I. Bloch, Phys. Rev. Lett. **93**, 073002 (2004).
[191] T. Volz, N. Syassen, D. M. Bauer, E. Hansis, S. Duerr, and G. Rempe, Nat. Phys. **2**, 692 (2006).
[192] C. Ospelkaus, S. Ospelkaus, L. Humbert, P. Ernst, K. Sengstock, and K. Bongs, Phys. Rev. Lett. **97**, 120402 (2006).
[193] D. DeMille, D. R. Glenn, and J. Petricka, Eur Phys J D **31**, 375 (2004).
[194] M. T. Hummon, W. C. Campbell, E. Tsikata, Y. Wang, and J. M. Doyle, arXiv **physics.atom-ph** (2008).
[195] B. C. Sawyer, B. K. Stuhl, D. Wang, M. Yeo, and J. Ye, Phys. Rev. Lett. **101**, 4 (2008).
[196] N. Vanhaecke, W. D. Melo, B. L. Tolra, D. Comparat, and P. Pillet, Phys. Rev. Lett. **89**, 063001 (2002).
[197] D. Wang, J. Qi, M. F. Stone, O. Nikolayeva, B. Hattaway, S. D. Gensemer, H. Wang, W. T. Zemke, P. L. Gould, E. E. Eyler, et al., Eur Phys J D **31**, 165 (2004).
[198] D. Gerlich, *State-Selected and State-to-State Ion-Molecule*

*Reaction Dynamics. Part 1: Experiment, Edited by Cheuk-Yiu Ng and Michael Baer. Advances in Chemical Physics Series, Vol. LXXXII.* (Wiley, New York, 1992).
[199] S. Willitsch, M. T. Bell, A. D. Gingell, and T. P. Softley, Phys. Chem. Chem. Phys. **10**, 7200 (2008).
[200] D. Gerlich, Phys. Scr. **T59**, 256 (1995).
[201] O. V. Boyarkin, S. R. Mercier, A. Kamariotis, and T. R. Rizzo, J Am Chem Soc **128**, 2816 (2006).
[202] J. Mikosch, U. Fruehling, S. Trippel, R. Otto, P. Hlavenka, D. Schwalm, M. Weidemüller, and R. Wester, Phys. Rev. A **78**, 023402 (2008).
[203] R. Otto, J. Mikosch, S. Trippel, M. Weidemüller, and R. Wester, Phys. Rev. Lett. **101**, 063201 (2008).
[204] K. Molhave and M. Drewsen, Phys. Rev. A **62**, 011401 (2000).
[205] A. Bertelsen, S. Jorgensen, and M. Drewsen, J Phys B-At Mol Opt **39**, L83 (2006).
[206] I. S. Vogelius, L. B. Madsen, and M. Drewsen, Phys. Rev. Lett. **89**, 173003 (2002).
[207] I. S. Vogelius, L. B. Madsen, and M. Drewsen, J Phys B-At Mol Opt **37**, 4571 (2004).
[208] I. S. Vogelius, L. B. Madsen, and M. Drewsen, Phys. Rev. A **70**, 053412 (2004).
[209] I. S. Vogelius, L. B. Madsen, and M. Drewsen, J Phys B-At Mol Opt **39**, S1267 (2006).
[210] L. Hornekaer, N. Kjaergaard, A. M. Thommesen, and M. Drewsen, Phys. Rev. Lett. **86**, 1994 (2001).
[211] B. Roth, P. Blythe, H. Daerr, L. Patacchini, and S. Schiller, J Phys B-At Mol Opt **39**, S1241 (2006).
[212] C. J. Myatt, E. A. Burt, R. W. Ghrist, E. A. Cornell, and C. E. Wieman, Phys. Rev. Lett. **78**, 586 (1997).
[213] I. Bloch, M. Greiner, O. Mandel, T. W. Hansch, and T. Esslinger, Phys. Rev. A **64**, 021402 (2001).
[214] G. Modugno, G. Ferrari, G. Roati, R. J. Brecha, A. Simoni, and M. Inguscio, Science **294**, 1320 (2001).
[215] M. Mudrich, S. Kraft, K. Singer, R. Grimm, A. Mosk, and M. Weidemüller, Phys. Rev. Lett. **88**, 253001 (2002).
[216] P. Soldan and J. M. Hutson, Phys. Rev. Lett. **92**, 163202 (2004).
[217] M. Lara, J. L. Bohn, D. Potter, P. Soldan, and J. M. Hutson, Phys. Rev. Lett. **97**, 183201 (2006).
[218] M. Lara, J. L. Bohn, D. E. Potter, P. Soldan, and J. M. Hutson, Phys. Rev. A **75**, 012704 (2007).
[219] P. S. Żuchowski and J. M. Hutson, Phys. Rev. A **78**, 9 (2008).
[220] J. van Veldhoven, H. L. Bethlem, and G. Meijer, Phys. Rev. Lett. **94**, 083001 (2005).
[221] P. Barletta, J. Tennyson, and P. F. Barker, Phys. Rev. A **78**, 4 (2008).
[222] S. Y. T. van de Meerakker, B. G. Sartakov, A. P. Mosk, R. T. Jongma, and G. Meijer, Phys. Rev. A **68**, 032508 (2003).
[223] M. G. Raizen, A. M. Dudarev, Q. Niu, and N. J. Fisch, Phys. Rev. Lett. **94**, 053003 (2005).
[224] G. N. Price, S. T. Bannerman, K. Viering, E. Narevicius, and M. G. Raizen, Phys. Rev. Lett. **100**, 093004 (2008).
[225] J. J. Thorn, E. A. Schoene, T. Li, and D. A. Steck, Phys. Rev. Lett. **100**, 240407 (2008).
[226] A. Marian and B. Friedrich, Nat Photonics **2**, 463 (2008).
[227] D. Meschede, W. Jhe, and E. A. Hinds, Phys. Rev. A **41**, 1587 (1990).
[228] H. W. Chan, A. T. Black, and V. Vuletić, Phys. Rev. Lett. **90**, 063003 (2003).
[229] A. T. Black, H. W. Chan, and V. Vuletić, Phys. Rev. Lett. **91**, 203001 (2003).
[230] G. Morigi, P. W. H. Pinkse, M. Kowalewski, and R. de Vivie-Riedle, Phys. Rev. Lett. **99**, 073001 (2007).
[231] B. L. Lev, A. Vukics, E. R. Hudson, B. C. Sawyer, P. Domokos, H. Ritsch, and J. Ye, Phys. Rev. A **77**, 023402 (2008).
[232] W. Lu, Y. Zhao, and P. F. Barker, Phys. Rev. A **76**, 013417 (2007).
[233] P. Staanum, S. D. Kraft, J. Lange, R. Wester, and M. Weidemüller, Phys. Rev. Lett. **96**, 023201 (2006).
[234] J. M. Hutson and P. Soldan, Int. Rev. Phys. Chem. **26**, 1 (2007).
[235] A. T. Grier, M. Cetina, F. Oručević, and V. Vuletić, arXiv **physics.atom-ph** (2008).
[236] M. T. Cvitas, P. Soldan, J. M. Hutson, P. Honvault, and J. M. Launay, Phys. Rev. Lett. **94**, 200402 (2005).
[237] E. P. Wigner, Phys Rev **73**, 1002 (1948).
[238] H. R. Sadeghpour, J. L. Bohn, M. J. Cavagnero, B. D. Esry, I. I. Fabrikant, J. H. Macek, and A. R. P. Rau, J Phys B-At Mol Opt **33**, R93 (2000).
[239] M. S. Child, *Molecular Collision Theory* (Dover, 1996).
[240] L. D. Landau and E. M. Lifshitz, *Quantum Mechanics: Non-relativistic Theory* (Pergamon, Oxford, 1977).
[241] J. Weiner, V. S. Bagnato, S. Zilio, and P. S. Julienne, Rev. Mod. Phys. **71**, 1 (1999).
[242] J. M. Hutson, New J. Phys. **9**, 152 (2007).
[243] A. Mody, M. Haggerty, J. M. Doyle, and E. J. Heller, Phys. Rev. B **64**, 085418 (2001).
[244] H. Bethe, Phys Rev **47**, 747 (1935).
[245] R. T. Skodje, D. Skouteris, D. E. Manolopoulos, S. H. Lee, F. Dong, and K. Liu, J. Chem. Phys. **112**, 4536 (2000).
[246] R. T. Skodje, D. Skouteris, D. E. Manolopoulos, S. H. Lee, F. Dong, and K. P. Liu, Phys. Rev. Lett. **85**, 1206 (2000).
[247] P. F. Weck and N. Balakrishnan, J. Chem. Phys. **122**, 164309 (2005).
[248] P. F. Weck and N. Balakrishnan, J. Chem. Phys. **123**, 144308 (2005).
[249] G. Quemener and N. Balakrishnan, J. Chem. Phys. **128**, 224304 (2008).
[250] P. F. Weck and N. Balakrishnan, Int. Rev. Phys. Chem. **25**, 283 (2006).
[251] T. Xie, D. Y. Wang, J. M. Bowman, and D. E. Manolopoulos, J. Chem. Phys. **116**, 7461 (2002).
[252] J. M. Bowman, Chem. Phys. **308**, 255 (2005).
[253] E. Bodo, F. A. Gianturco, N. Balakrishnan, and A. Dalgarno, J Phys B-At Mol Opt **37**, 3641 (2004).
[254] R. V. Krems, Phys. Rev. Lett. **93**, 013201 (2004).
[255] A. V. Avdeenkov and J. L. Bohn, Phys. Rev. Lett. **90**, 043006 (2003).

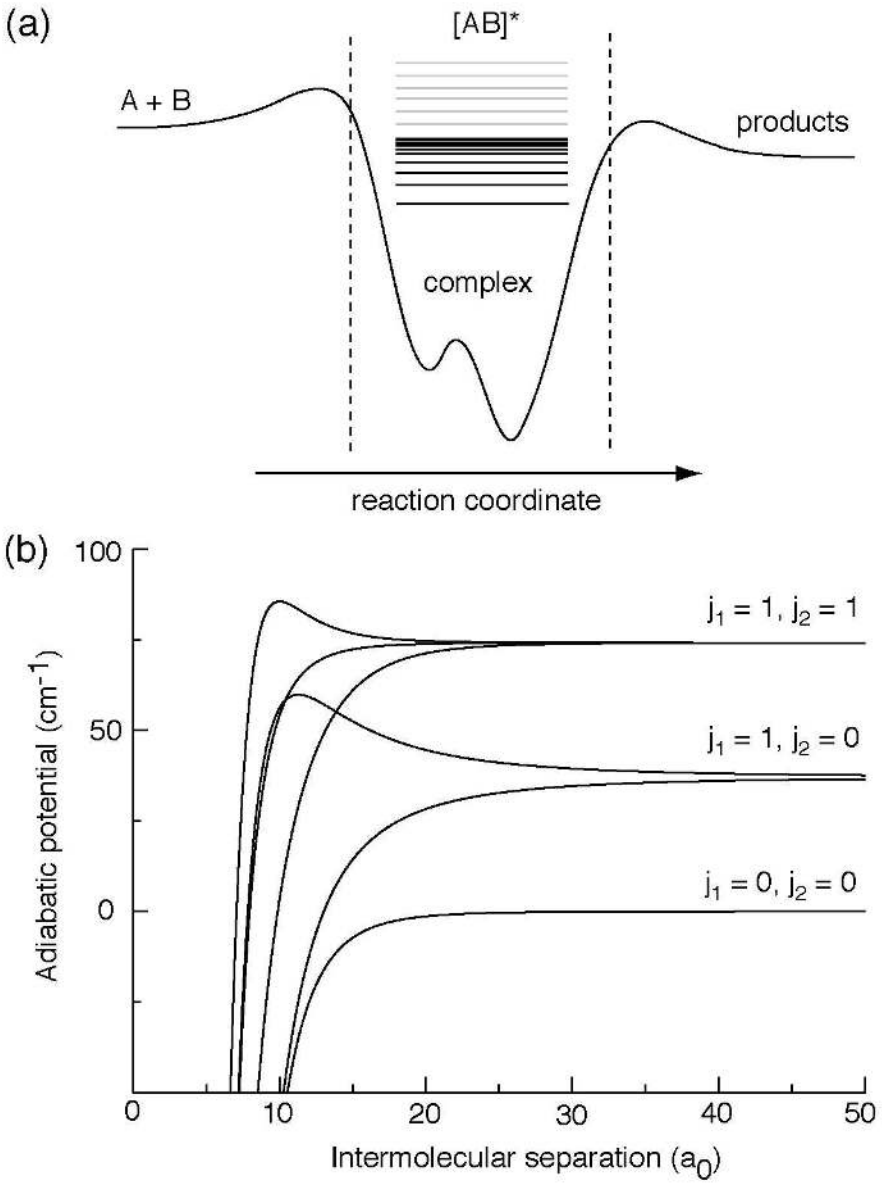


155x201mm (200 x 200 DPI)

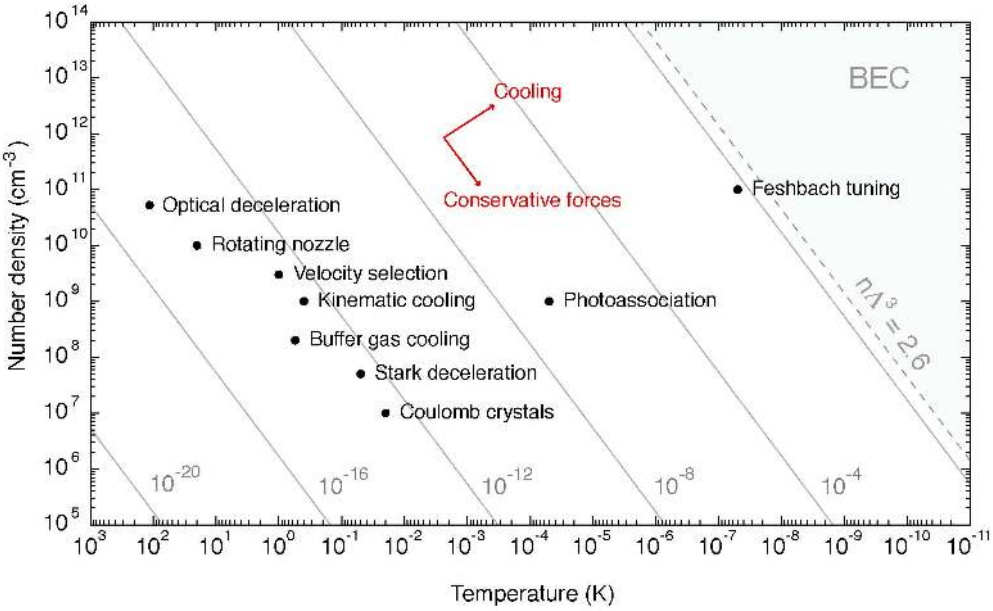


279x172mm (200 x 200 DPI)

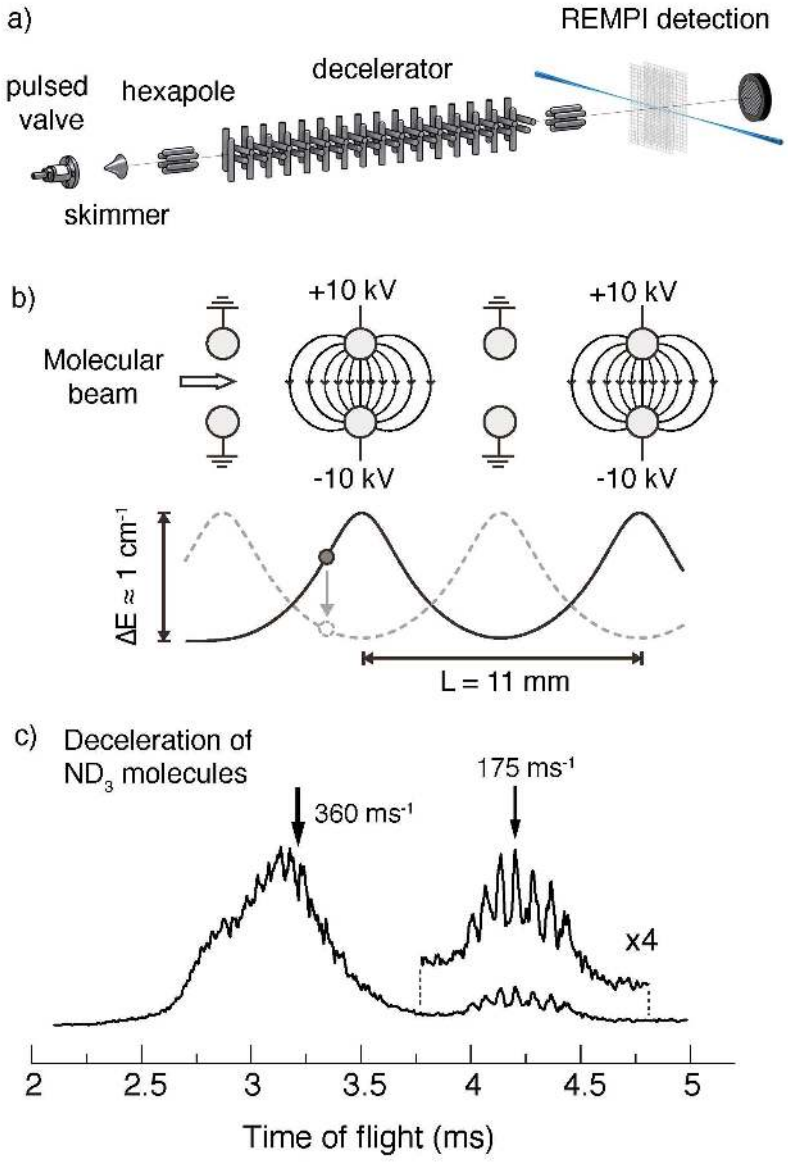


83x121mm (486 x 484 DPI)

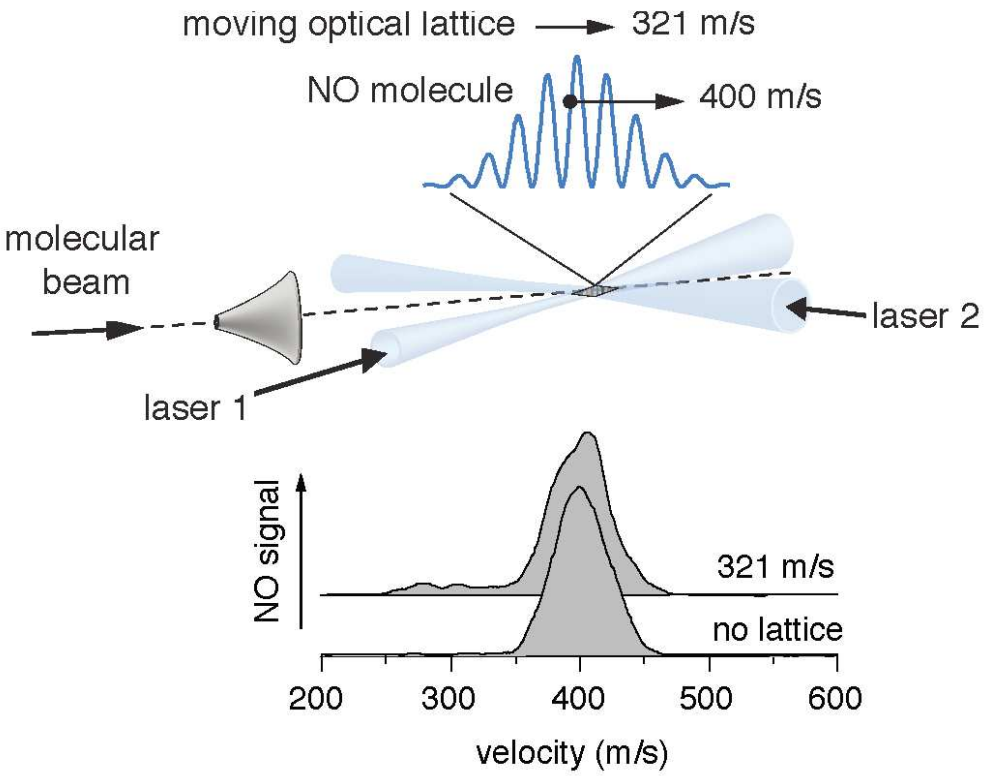


131x105mm (200 x 200 DPI)

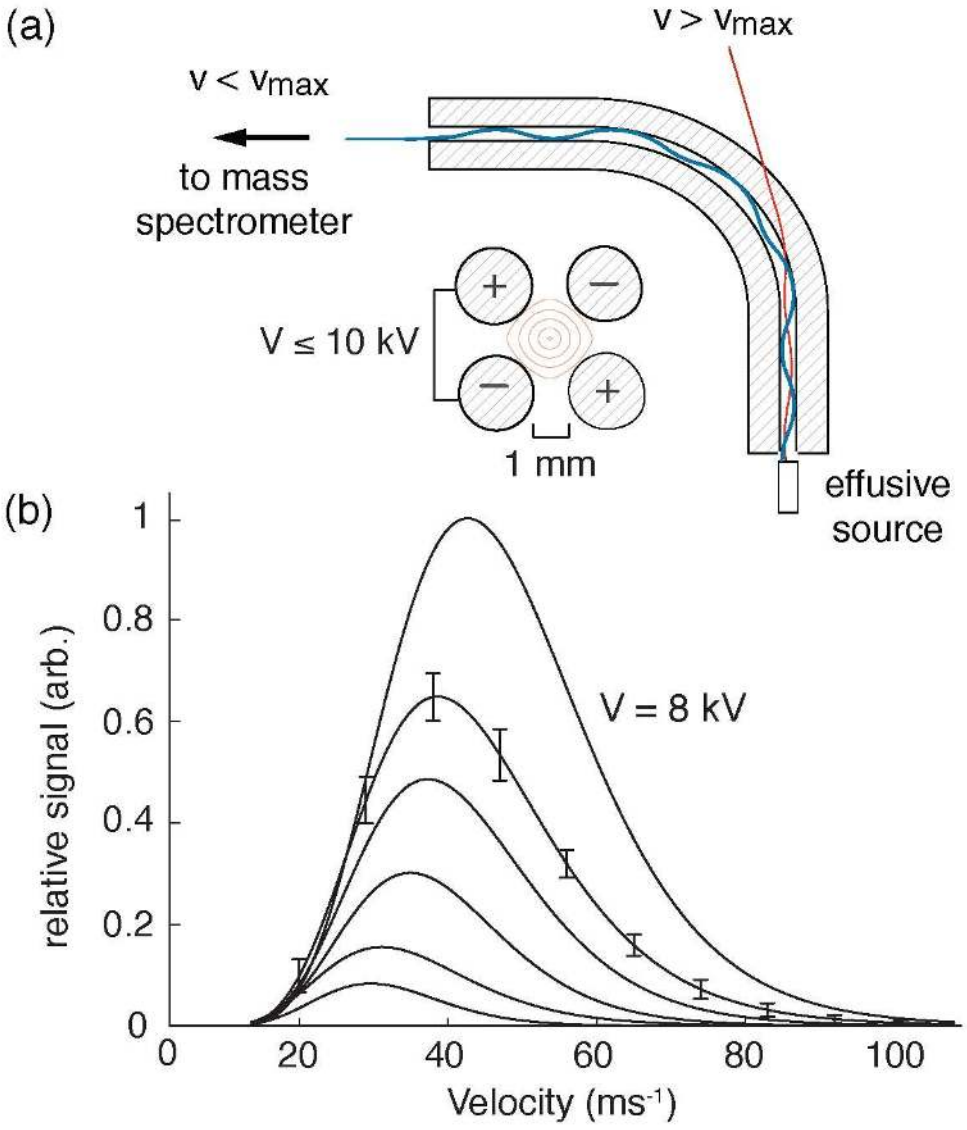


152x177mm (200 x 200 DPI)

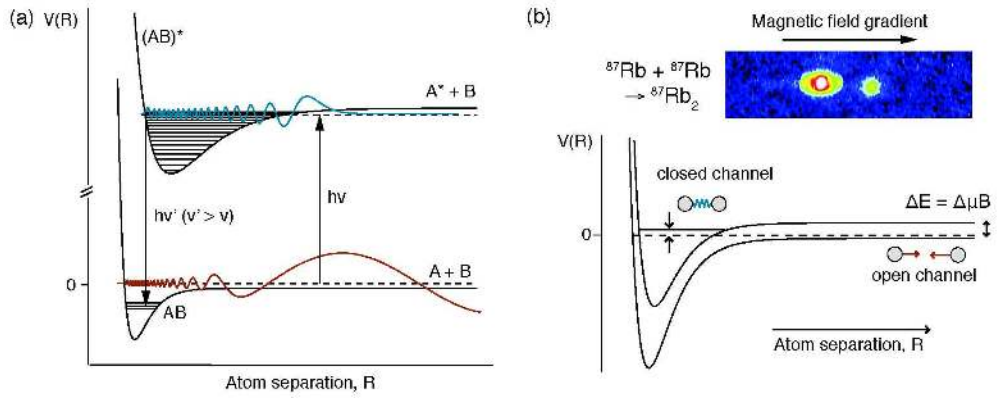


201x80mm (222 x 222 DPI)

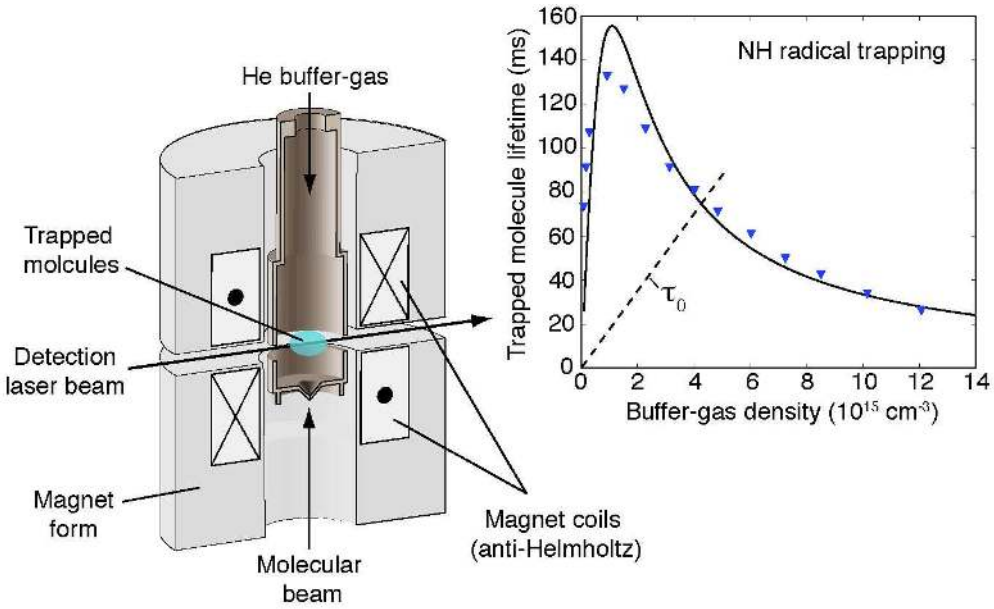


174x105mm (200 x 200 DPI)

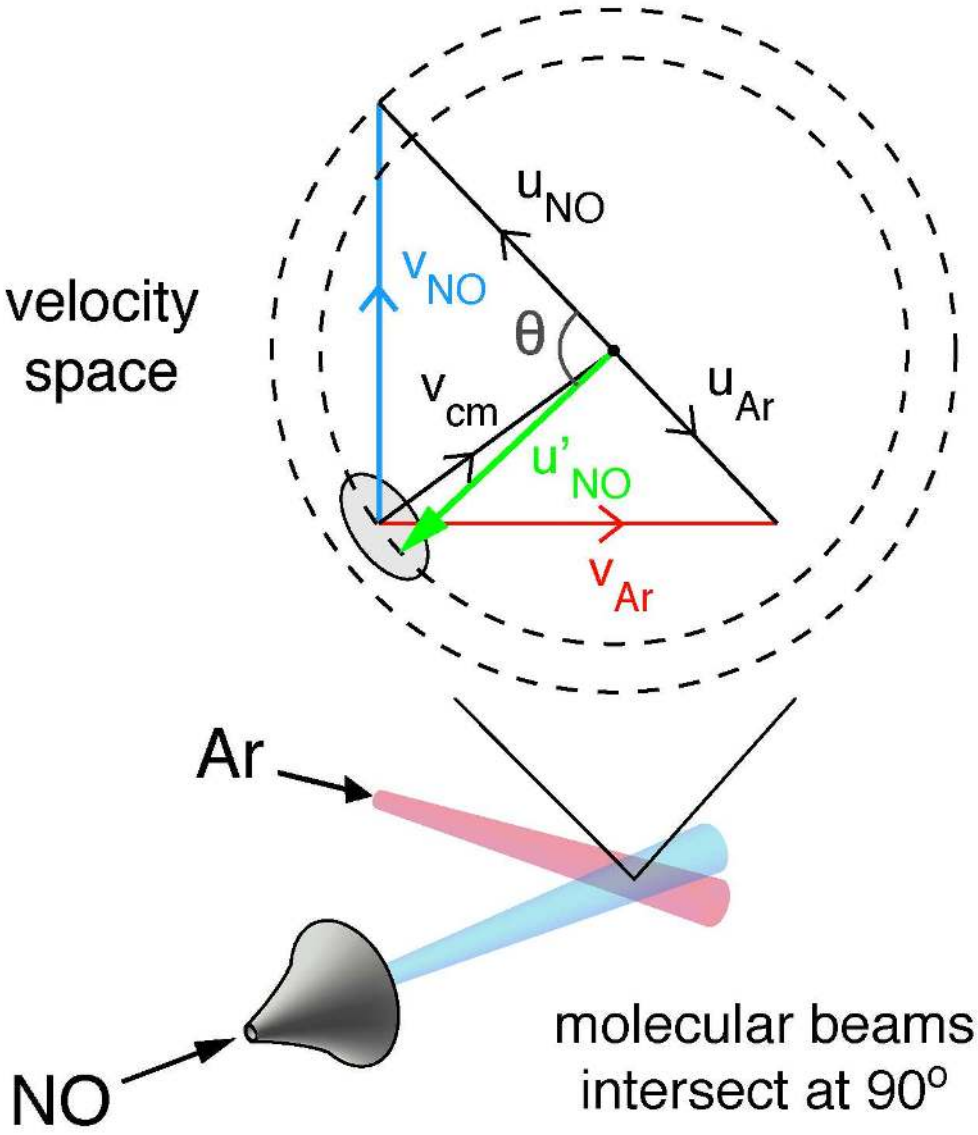


163x191mm (200 x 200 DPI)

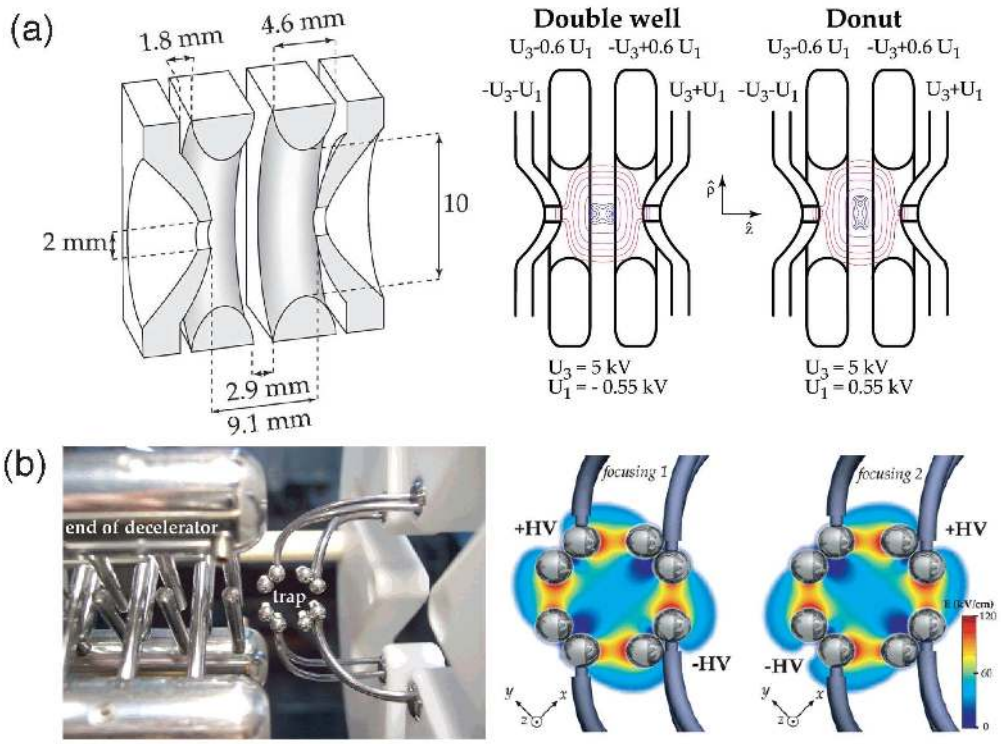


201x152mm (249 x 249 DPI)

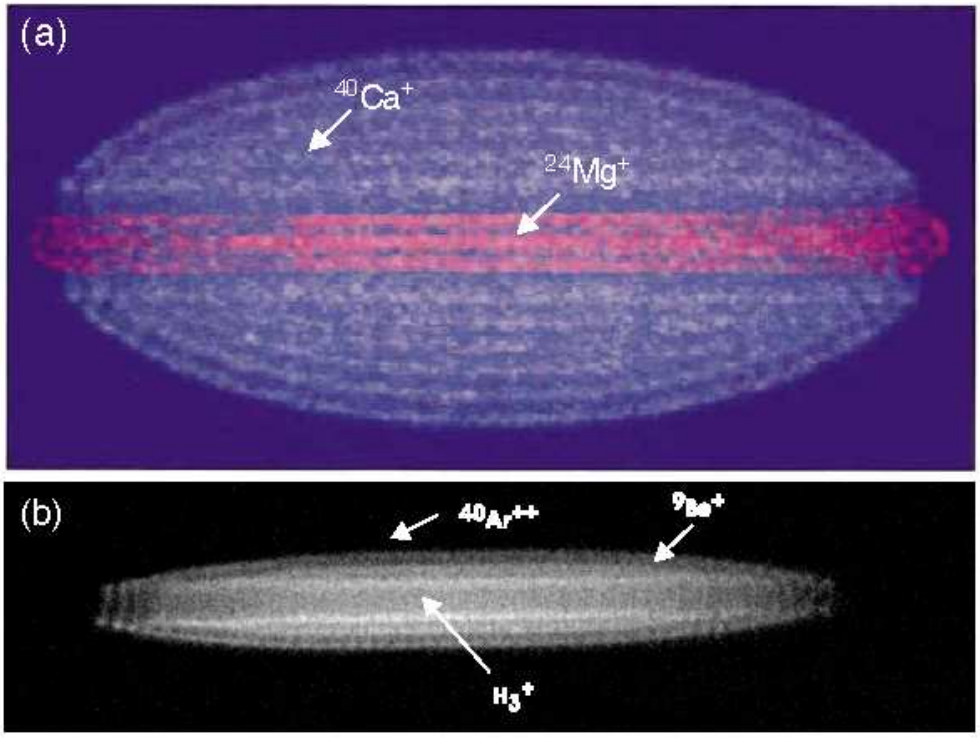


83x64mm (181 x 181 DPI)

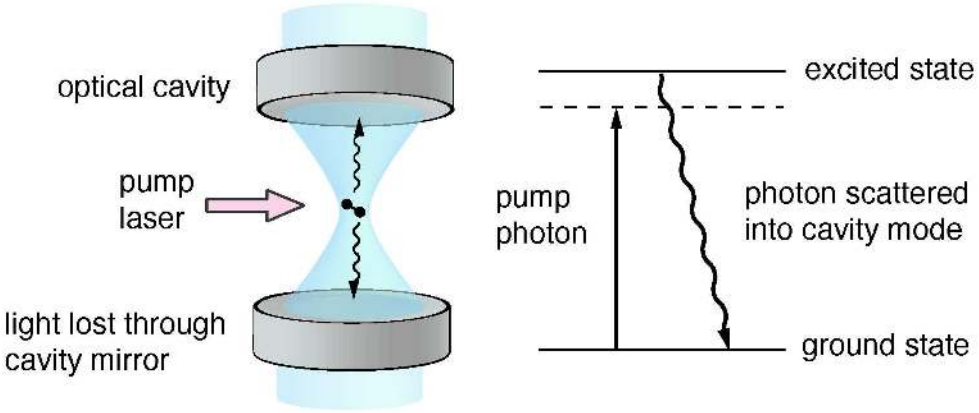


239x103mm (200 x 200 DPI)

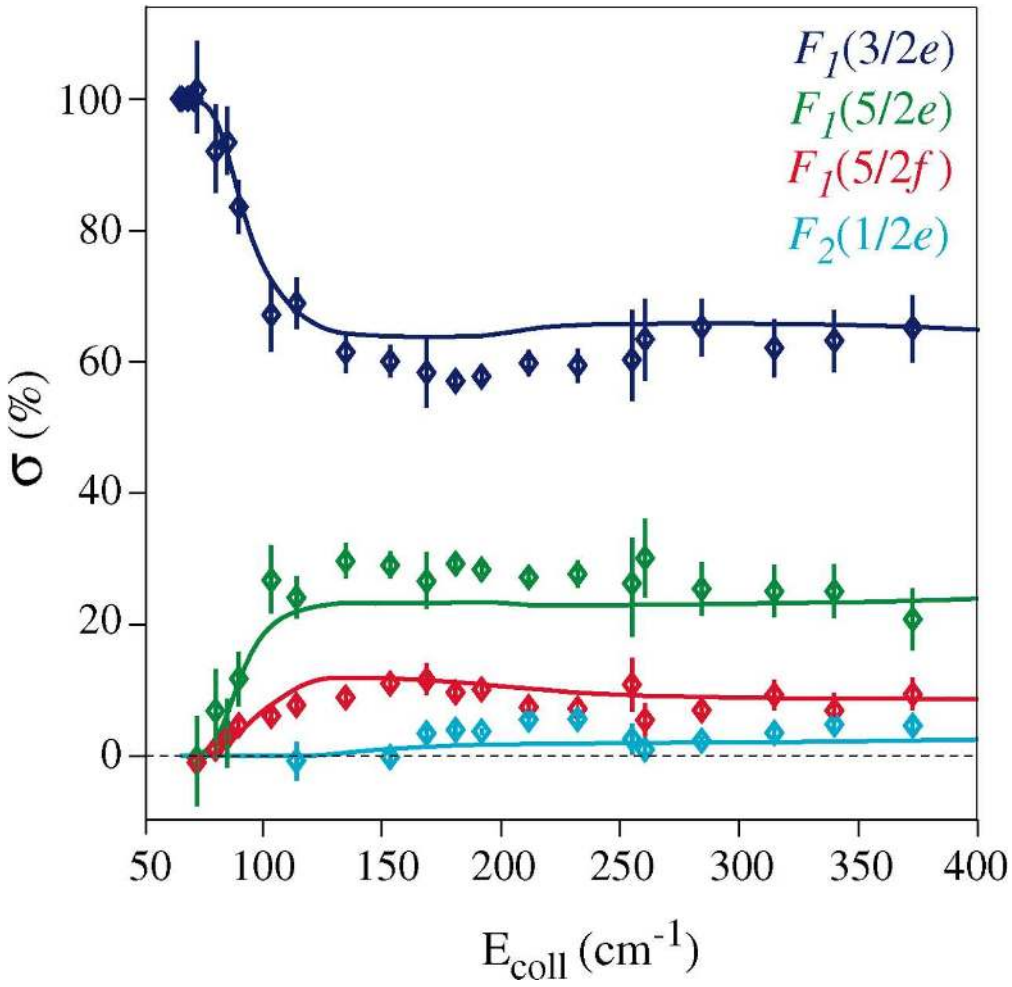


451x440mm (72 x 72 DPI)

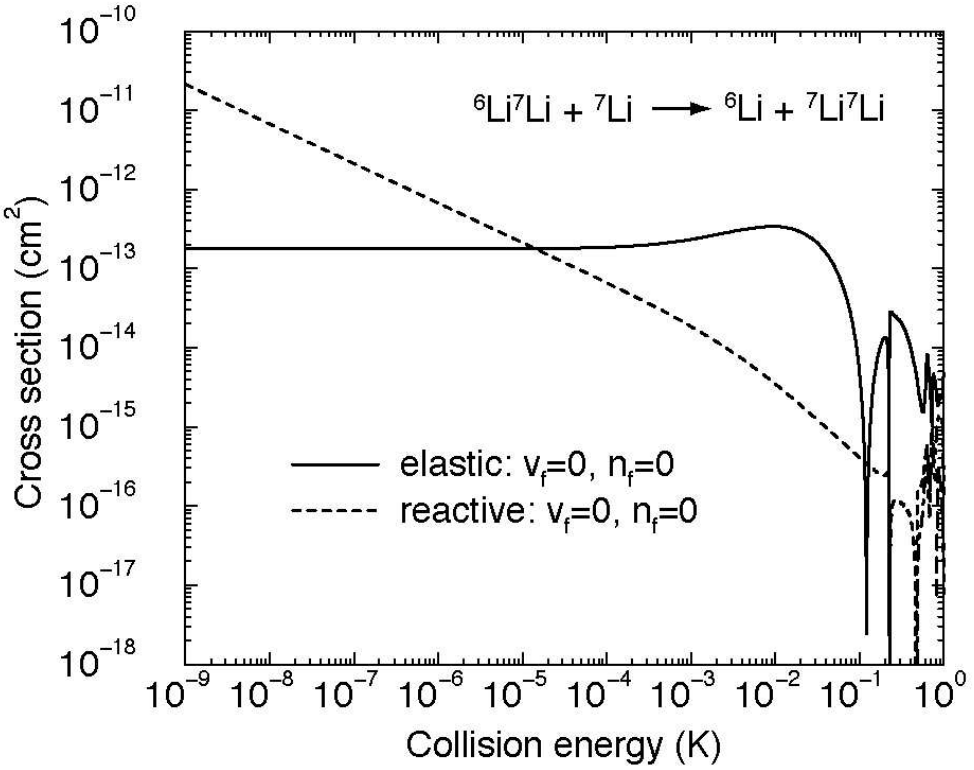


119x96mm (200 x 200 DPI)

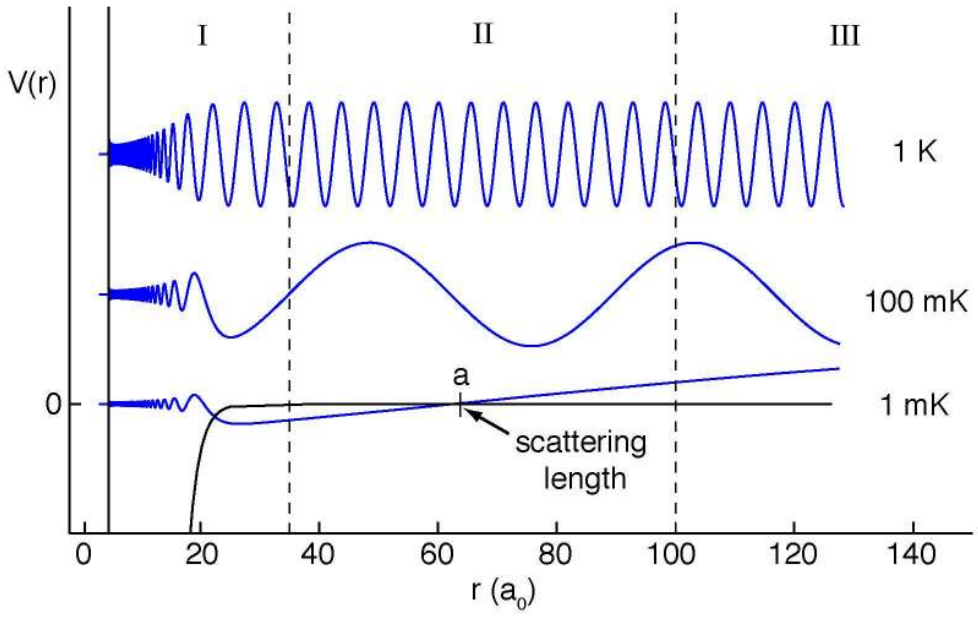


207x132mm (200 x 200 DPI)